NUREG/CR–4055
SAND84–1144
R7
Printed December 1984

The D10 Experiment: Coolability of UO_2 Debris in Sodium With Downward Heat Removal

G. W. Mitchell, C. A. Ottinger, H. Meister

Prepared by
Sandia National Laboratories
Albuquerque, New Mexico 87185 and Livermore, California 94550
for the United States Department of Energy
under Contract DE-AC04-76DP00789

Prepared for
U. S. NUCLEAR REGULATORY COMMISSION

Available from

GPO Sales Program
Division of Technical Information and Document Control
U.S. Nuclear Regulatory Commission
Washington, D.C. 20555

and

National Technical Information Service
Springfield, Virginia 22161

NUREG/CR-4055
SAND84-1144
R7

THE D10 EXPERIMENT: COOLABILITY OF UO_2 DEBRIS IN SODIUM WITH DOWNWARD HEAT REMOVAL*

G. W. Mitchell
C. A. Ottinger
Sandia National Laboratories
Albuquerque, New Mexico 87185

H. Meister
EURATOM Joint Research Center
Ispra, Italy

December 1984

Sandia National Laboratories
Albuquerque, New Mexico 87185
Operated by
Sandia Corporation
for the
U.S. Department of Energy

Prepared for
Office of Nuclear Regulatory Research
U.S. Nuclear Regulatory Commission
Washington, D.C. 20555
NRC FIN A-1181

---

* This work was supported by the U.S. Nuclear Regulatory Commission, EURATOM JRC and the Japanese PNC and performed at Sandia National Laboratories, which is operated for the U.S. DOE under contract number DE-AC04-76DP00789.

ABSTRACT

The LMFBR Debris Coolability Program at Sandia National Laboratories investigates the coolability of particle beds which may form following a severe accident involving core disassembly in a nuclear reactor. The D series experiments utilize fission heating of fully enriched UO_2 particles submerged in sodium to realistically simulate decay heating. The D10 experiment is the first in the series to study the effects of bottom cooling of the debris that could be provided in an actual accident condition by structural materials onto which the debris might settle. Additionally, the D10 experiment was designed to achieve maximum temperatures in the debris approaching the melting point of UO_2. The experiment was successfully operated for over 50 hours and investigated downward heat removal in a packed bed at specific powers of 0.16 to 0.58 W/g. Dryout in the debris was achieved at powers from 0.42 to 0.58 W/g. Channels were induced in the bed and channeled bed dryout was achieved at powers of 1.06 to 1.77 W/g. Maximum temperatures in excess of 2500°C were attained.

CONTENTS

LIST OF ILLUSTRATIONS

LIST OF TABLES

ACKNOWLEDGMENT

The successful operation of the D10 experiment was preceded by a period of concept formulation, design engineering, hardware testing, component fabrication and assembly of the experiment. A large number of individuals were involved in the project during this time and deserve substantial recognition for their work. J. Gronager, K. Takahashi (PNC), and G. Fieg (KfK) initiated the preliminary concepts and design, including fabrication and operation of a full-scale systems test of the experiment, which contributed substantially to subsequent design efforts. Fabrication of many complex experimental components was ably guided by K. Gawith. The efforts of R. Gomez during fabrication and assembly and of J. Reinhart and H. Heerdt during final preparation and operation were essential to the success of the experiment. Thanks also to R. Lipinski, J. Kelly, K. Mehr (JRC Ispra), and L. Barleon (KfK) for their insight, analyses, and contributions prior to and during operation of the experiment. Finally, thanks to T. Schmidt and J. Walker for their support and supervision during difficult times.

THE D1O EXPERIMENT: COOLABILITY OF UO_2 DEBRIS IN SODIUM WITH DOWNWARD HEAT REMOVAL

1. INTRODUCTION

The LMFBR Debris Coolability Program at Sandia National Laboratories (SNL) investigates the coolability of particle beds that may form following a severe accident involving core disassembly in a nuclear reactor. This debris is capable of generating significant power through the decay of fission products. If the debris is flooded with coolant, heat removal can occur by conduction, convection, and boiling of the coolant. If the decay heat power is sufficiently high, dryout may occur, preventing the entry of liquid into regions of the bed. Because heat removal is then limited to conduction by solid UO_2 and vapor phases and by radiation, the temperatures in the dry regions of the bed increase considerably, which may threaten underlying structural components.

The Debris Coolability Program is a USNRC, Joint Research Center Ispra (EURATOM), and Power Reactor and Nuclear Fuel Development Corporation of Japan (PNC) jointly sponsored series of experiments designed to investigate the coolability of fragmented reactor materials. The D series experiments utilize fission heating of fully enriched UO_2 particles in the Annular Core Research Reactor (ACRR) to realistically simulate decay heat. Sodium is used as the coolant to study the effects of liquid subcooling with a high-conductivity fluid. The experiments conducted to date have investigated the parameters of bed depth, subcooling, particle size distribution, and stratification (1-5). The debris has been insulated on the sides and the bottom to allow one-dimensional analysis of the results. Additionally, tests accomplished to date have been limited to maximum temperatures of about 1200°C based on the utilization of conventional materials. Although these experiments are directed primarily toward Liquid Metal Fast Breeder Reactor (LMFBR) safety questions, the coolability models that have been developed based on these experiments are applicable to both sodium- and water-cooled reactors.

The D1O experiment is the first in the series to study the effects of bottom cooling that might be provided by structural materials onto which the reactor debris might settle in an accident condition. It was designed to achieve temperatures in the debris approaching the melting point of UO_2 to investigate any change in coolability that might occur at those temperatures. These objectives were successfully met during the experiment, which was operated for a period of over 53 hr. Downward cooling was investigated under subcooled, packed bed, and channeled bed conditions. Packed bed and channeled bed dryout powers were determined under several downward cooling

conditions. Extended dryouts were established with maximum temperatures in the bed of 2500°C.

This report is intended to be primarily a description of the operation of the experiment and a compilation of the data. Only limited interpretation and analysis of the results are provided.

2. EXPERIMENT DESCRIPTION

2.1 Experimental Objectives

The primary objective of the D series experiments is to provide a data base for the development and validation of models that can be used to assess reactor safety. Thus, the experiments cover as wide a parameter space as possible and attempt to identify the important phenomena that govern coolability. The D10 experiment was originally proposed in 1979 as the first inpile experiment investigating debris coolability that would include the effects of bottom cooling of the debris. This would simulate the cooling that could be provided by structural components onto which the debris might settle in an accident. The objectives of the experiment were later expanded to include the investigation of effects that might be induced at high temperatures as the debris approaches UO_2 melt. Based on these objectives, the experiment was designed to study the coolability of a bed of UO_2 particles in sodium, 160 mm high and 102 mm in diameter, which could be fission-heated in the ACRR to a maximum temperature of 2500°C and a maximum power of about 2.0 W/g in the UO_2.

To achieve these objectives, temperatures were recorded at different power levels to study various regimes of heat removal that might exist in such a bed. Power required to produce incipient dryout at various rates of downward cooling were determined during the experiment. In addition, the thermal conductivity of dry debris in the presence of sodium vapor at power levels above that required for incipient dryout can be determined based on measured temperatures.

2.2 Experiment Design

The design approach of the D10 experiment was based on the experimental objectives and the safety requirements for operating such experiments in the ACRR. An overall layout of the experiment installed in the ACRR is shown in Figure 1. The experiment section, consisting of the lower 200 cm of the assembly installed in the 23-cm-diameter dry central cavity of the ACRR is shown in Figure 2. Two independent gas cooling loops were used to remove energy from both the sodium pool overlying the debris and the bottom of the bed. Two independent radiological containments were provided to meet ACRR safety requirements for the containment of fission products generated during the experiment. The bed was contained in a crucible side-insulated to provide an approximate one-dimensional geometry for analysis and to insulate the containment barriers from the high debris bed temperatures expected during the experiment. Instrumentation, consisting of thermocouples and ultrasonic thermometers (UTs), was placed in the experiment to minimize perturbations that would adversely affect the data but in sufficient quantity to obtain the data necessary to characterize bed behavior.

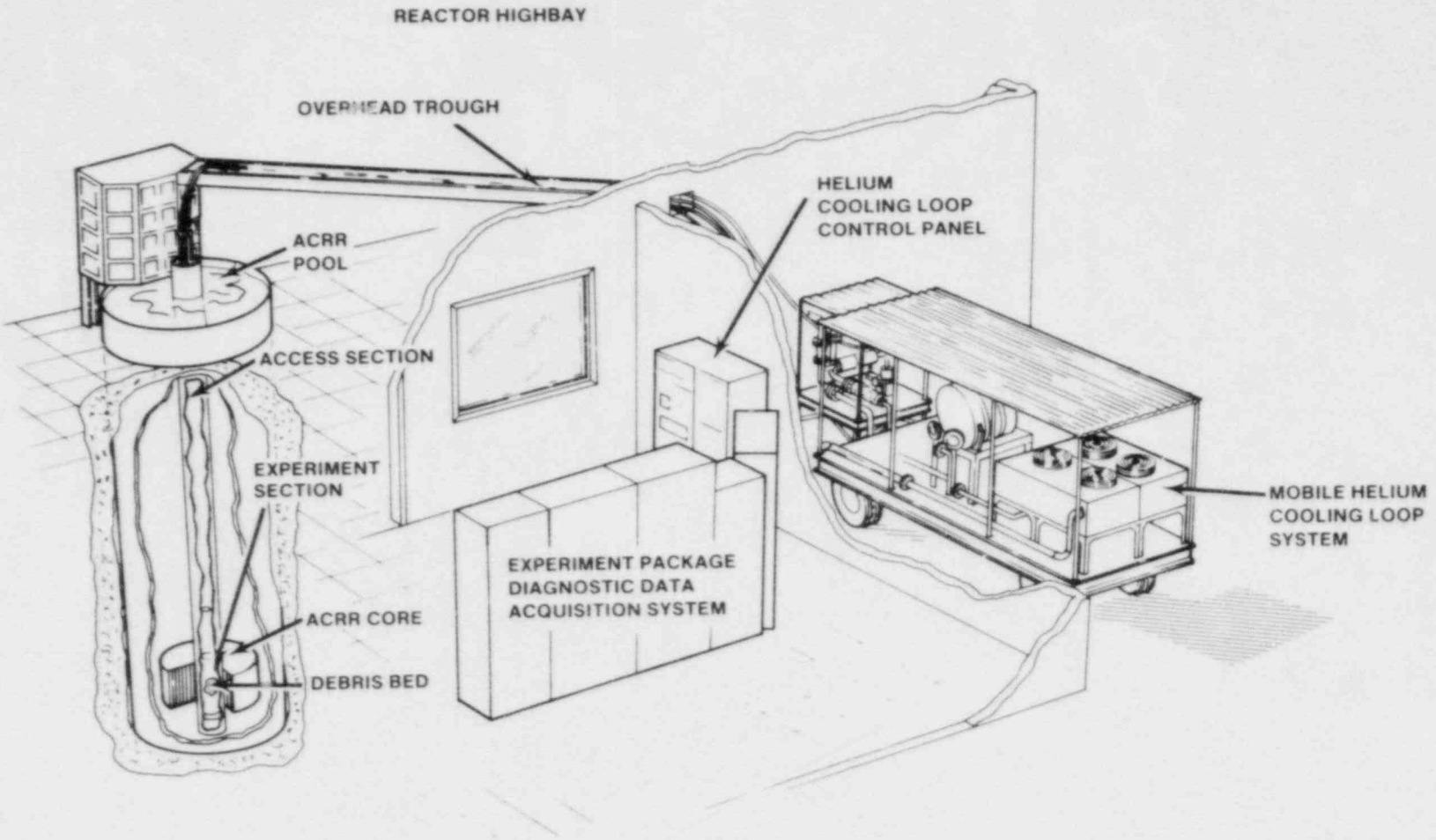

Figure 1. D10 Experiment Layout

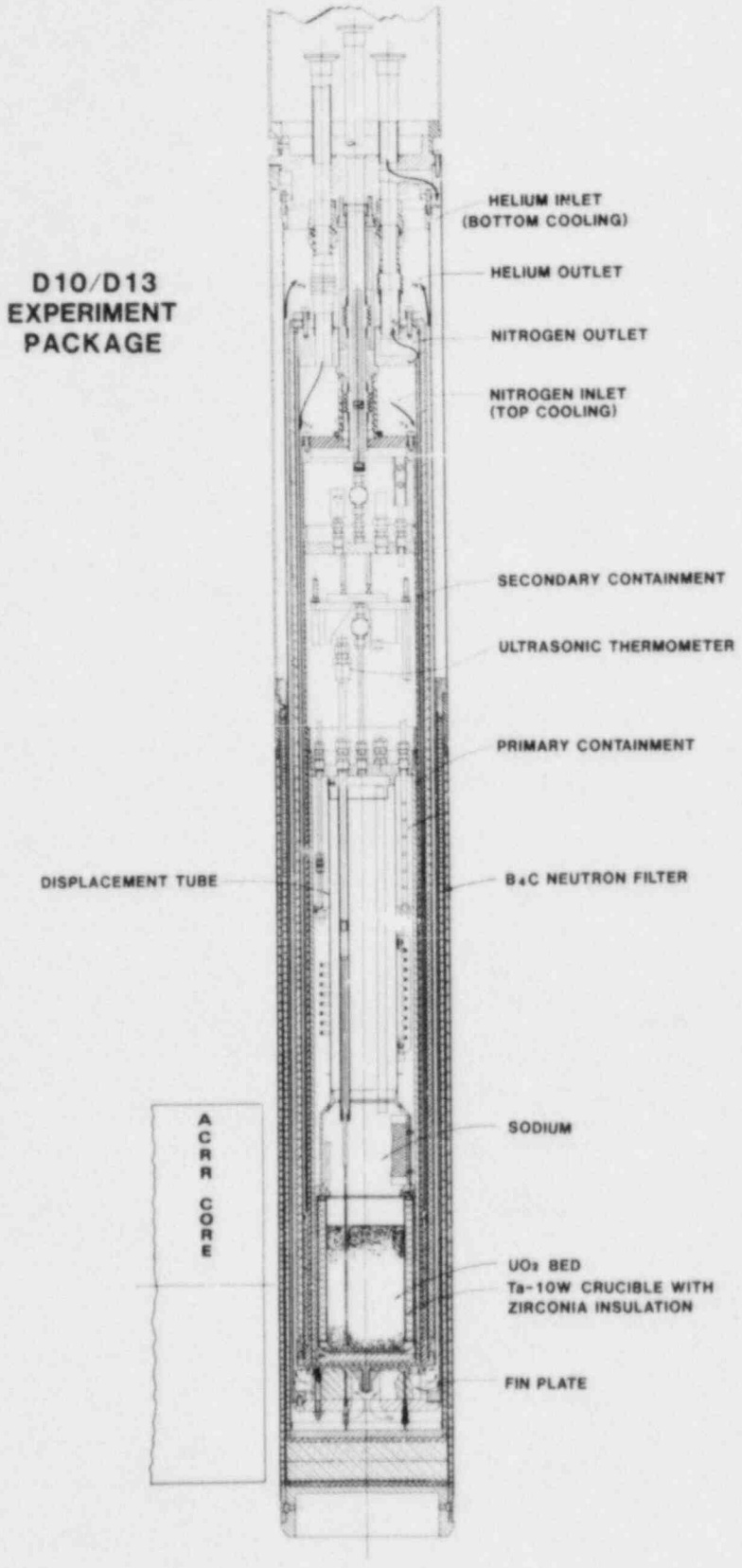

Figure 2. Experiment Section

2.2.1 Containment Description

The containment vessels for the D10 Experiment provide radiological barriers to the release of fission products during the experiment and are basically closed-end cylinders. Design drawings of the containment structures are included in Appendix A. The containment vessels were required to contain sodium at the maximum sodium temperature of 600°C. Higher temperatures would exist at the bottom of the containment vessels due to heat losses from the debris bed. SS 304 was selected as the principal containment material based on availability and ease of fabrication. Structural evaluations were performed in conjunction with two-dimensional thermal evaluations to determine maximum allowable operating temperatures (6,7). These evaluations indicated that maximum temperatures would exist on the lower containment structures during periods of low downward cooling. Temperatures between 700° and 780°C could be allowed if the pressures imposed on the containments were maintained below predetermined limits. The upper part of the primary containment could experience a temperature as high as the liquid sodium temperature of 600°C while the top of the secondary containment was not expected to exceed 300°C. To improve heat removal from the sodium through the cylinder walls, the 0.75-mm gap between the two containment cylinders was filled with copper powder and helium gas. To effect downward heat removal, the bottom plates of the two containment vessels were brazed to each other with Nioro (MP 950°C). A copper fin plate was bolted to the exterior surface of the secondary containment. Helium coolant passed through slots machined in the copper plate (Figure 3).

All penetrations in the primary containment were made with Swagelok seals welded or brazed into the 12-mm-thick cover plate, providing a continuous metallic, sodium-compatible containment barrier. All metallic-sheathed instrumentation in the primary containment was brazed into larger diameter feedthroughs with Nicrobraze, a high-temperature nickel-chrome braze. Secondary containment instrumentation penetrations were made using feedthroughs developed at SNL. These Swagelok compatible feedthroughs utilize glass-to-metal seals that have been tested for hermeticity after exposure to sodium in various thermal environments.

2.2.2 Cooling Systems

To control the temperature of the liquid sodium in the primary containment, the cylinders were cooled by a once-through flow of nitrogen that could be varied from 0.0 to about 70 g/s. The flow was directed by an upper manifold down an outer annulus and then up past the containment cylinders (Figure 2). Pressurized nitrogen gas in standard gas bottles was stepped down from the 170-bar supply pressure to about 4 bars by a two-stage pressure reduction system. An electrically operated variable position control valve was then used to regulate the

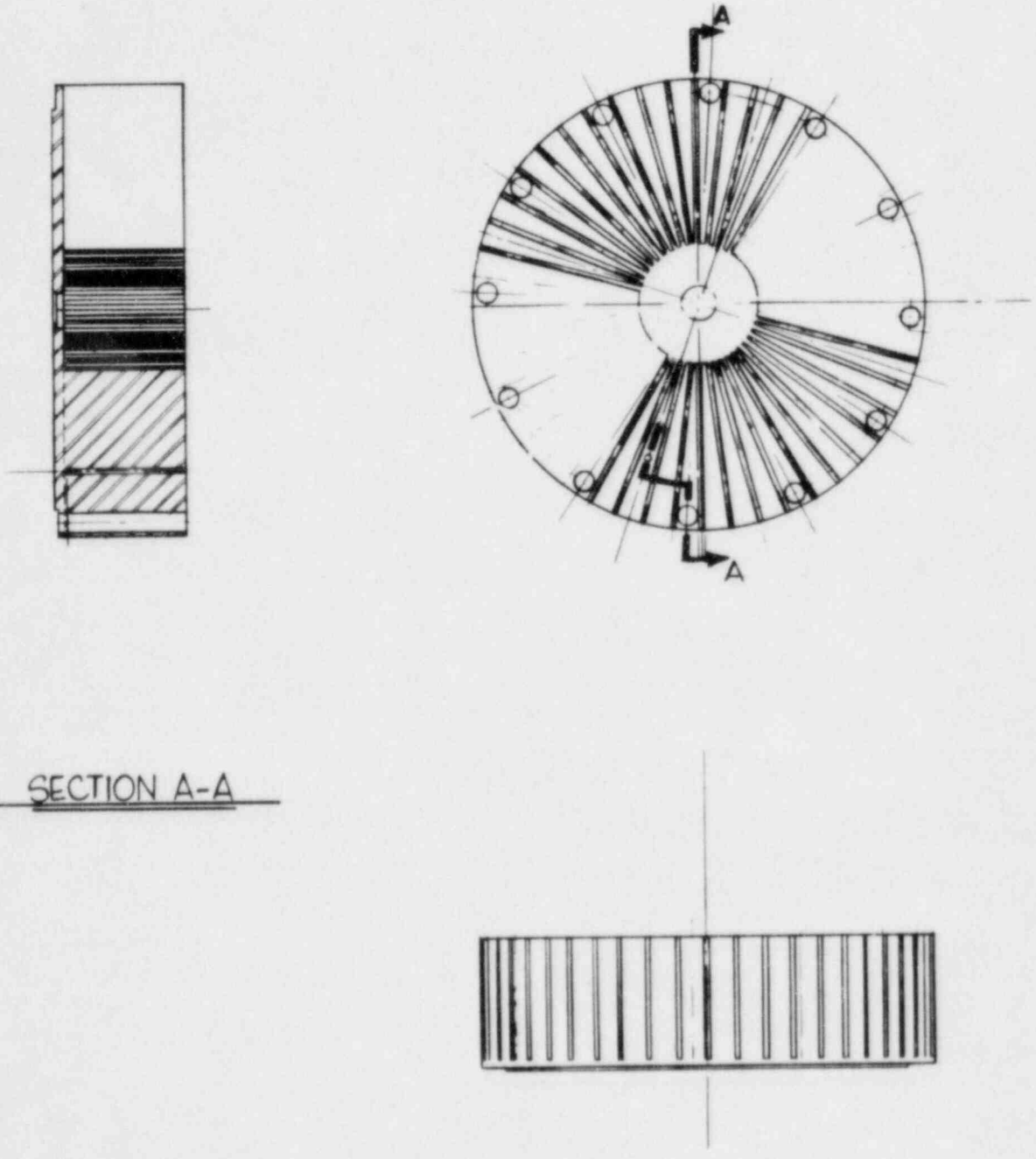

Figure 3. Copper Fin Plate

nitrogen flow to the experiment. The nitrogen flow passed through an HEPA filter prior to being discharged to the atmosphere at 0.8 bar. When experiment power was insufficient to maintain a desired sodium temperature, internal Inconel-sheathed electrical heaters rated at 4 kW were used to supplement fission-generated power. These heaters were also used to melt the sodium prior to nuclear heating.

A closed loop helium system used in previous debris bed experiments was used to supply helium coolant for bottom cooling (1-3). Flow rate was varied using an electrically operated three-way valve from 0.0 to ~20 g/s at a maximum pressure of 3.3 bars. During most of the D10 experiment, the system was operated at a pressure of about 2 bars. The helium flow path was outside that of the nitrogen, through the copper fin plate, and back up to the upper manifold. The helium and nitrogen cooling flows were separated by a 0.6-cm-thick layer of MinK blanket insulation. An additional layer of insulation separated the helium flow from the boron carbide neutron filter on the outer diameter of the experiment, which generated heat due to (n,α) reactions.

2.2.3 Experiment Operating Pressures

Previous debris bed experiments have been operated at pressures that ranged from 0.2 bar (D7, D9) to about 1.3 bars (D6). For radiological safety, the experiment containments are sealed throughout the experiment. The pressure is therefore thermodynamically related to the initial fill pressure and cannot be externally regulated during the experiment. The pressure of the cover gas overlying the sodium is the principal determinant of the sodium saturation temperature and therefore the sodium subcooling, which is an important experimental parameter. Low cover gas pressures have been used in several experiments to extend the range of sodium subcooling, which was studied or to decrease the maximum containment or crucible temperatures.

Since the D10 experiment incorporated a crucible that insulated the containments from the high-temperature debris, a substantial amount of flexibility existed in the selection of operating pressure. To be as prototypic as possible, pressures of about 2 bars would be desirable. Pressures significantly greater than 1 bar would, however, begin to impose undesirable loads on the containment structure, which would decrease the maximum allowable operating temperature. A nominal operating pressure near 1 bar was therefore selected for the D10 experiment. Since pressure varies with sodium temperature due to expansion of the sodium and heatup of the cover gas, the operating pressure was set to vary from about 0.8 bar at a sodium temperature of 350°C to 1.3 bars at a sodium temperature of 600°C. Corresponding sodium saturation temperatures ranged from 860° to 915°C.

To minimize pressure loads on the primary containment structure and to enhance the safety of the experiment, the pressure in the secondary containment was set to operate at a pressure slightly above that of the primary. The pressure in the secondary containment during the experiment varied from about 1.2 bars up to about 2.2 bars. Except for the safety considerations, this pressure did not play a role in the operation of the experiment, nor did it affect the data that were related only to the primary system pressure.

2.2.4 Crucible

The purpose of the crucible in the D10 experiment was to contain the UO_2 particles, insulating the containment walls from the high temperatures expected in the bed. Additionally, the side insulation reduced radial heat losses in the bed to approximate a one-dimensional condition for analysis of coolability phenomena. The goal to achieve high temperatures in the debris eliminated all steel and nickel alloys from consideration as crucible materials and required the consideration of refractory metal or ceramic materials. In addition to high temperatures, the crucible had to be compatible with sodium at high temperatures and had to be capable of withstanding significant thermal gradients. An extensive materials compatability program was undertaken to select a crucible material capable of containing the hot UO_2 debris and compatible with sodium liquid and vapor (8). A major uncertainty in this evaluation was the oxygen potential to which the material would be exposed during the experiment.

Based on the results of the materials evaluation, Ta-10W, T-111 (Ta-8W-2Hf), and Mo-41Re were identified as candidate crucible materials (9). Ta-10W was selected as the crucible material based on fabricability and availability in the U.S. Extensive thermal and structural evaluations of the crucible were also performed as part of the final design process to ensure that the crucible would perform its intended function of providing well-defined boundary conditions during the experiment (7,10). The double-walled crucible was fabricated by deep drawing two single-walled crucibles of Ta-10W with inner diameters of 10.2 cm and 12.4 cm (Figure 4). The walls of these crucibles were machined after drawing to a thickness of 0.15 to 0.16 cm and were then electron beam-welded to a machined closure with type ZYC zirconia insulation inserted between the walls. This insulation, obtained from the Zircar Corporation, was fabricated with a 91% nominal porosity and a published thermal conductivity in air of 0.0023 W/cm-K at 1650°C, its maximum continuous service temperature (11). The crucible was vented to the containment cover gas of 97.5% argon and 2.5% helium. A gas mixture primarily of argon was used to minimize the conductivity of the insulation, while a small quantity of helium was added to allow leak checks during assembly. Further, a small (less than 0.04 bar) sodium vapor pressure would exist due to the presence of sodium in the

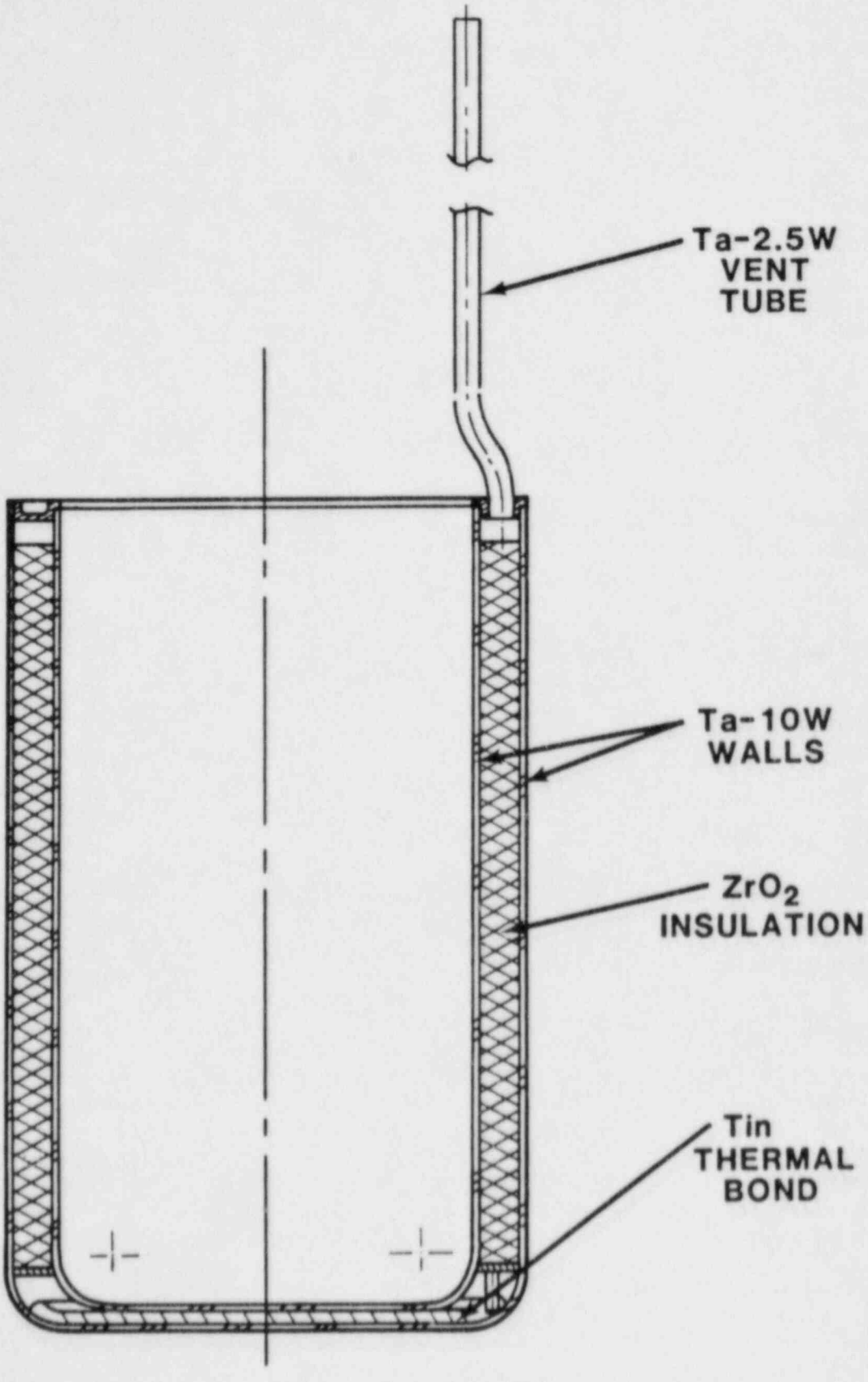

Figure 4. Crucible

primary containment. A liquid tin thermal bond between the metallic walls forming the bottom of the crucible provided a heat transfer path for downward cooling of the bed. To avoid any mechanical attachments, the crucible was supported in the experiment from below by a steel structure. The bed, crucible, and structure were submerged in a liquid sodium pool inside the primary containment.

2.2.5 Instrumentation

Instrumentation capable of measuring the maximum temperatures expected in the bed also had to be developed to achieve the experimental objectives. At the time the project was initiated, there was no instrumentation that would reliably measure temperatures above 1800°C under the severe restrictions imposed by requirements to provide two independent radiological containment barriers capable of operating in a 600°C liquid sodium environment (12). These restrictions required extensive development and testing to design conditions to ensure reliable operation during the experiment.

2.2.5.1 High-Temperature Thermocouples

Based on experience gained in fabricating a fuel centerline thermocouple capable of operating at 2200°C (13), Hanford Engineering Development Laboratory (HEDL) was contracted to fabricate sodium-compatible thermocouples capable of operating at 2300°C. They were successful in producing thermocouple assemblies accurate to within ±1% after operating for 50 hr at a maximum temperature of 2300°C. These assemblies were later qualified for operation at a maximum temperature of 2400°C. Development of these thermocouples was reported by HEDL in reference 14.

The rhenium-sheathed thermocouples consisted of tungsten 5/26 rhenium thermoelement wire with high-purity hafnia insulators manufactured by National Beryllia Corporation. The rhenium sheaths provided a hermetic boundary for the thermocouples at high temperature and in a sodium vapor environment. Ultramet fabricated the sheaths using the CVD process, with a wall thickness of 0.25 mm. Details of the thermocouple sheath, which extended into the debris bed and the thermoelement junction, are shown in Figure 5.

The rhenium sheath of each thermocouple was joined to a steel-sheathed extension cable that fed the thermoelement wire out of the experiment. The thermocouples were incorporated into assemblies of four, which were brazed into feedthroughs to maintain the required containment barriers. These assemblies were required to operate in an environment of sodium liquid and vapor and therefore were fabricated from SS 304, nickel alloys, and Nicrobraze.

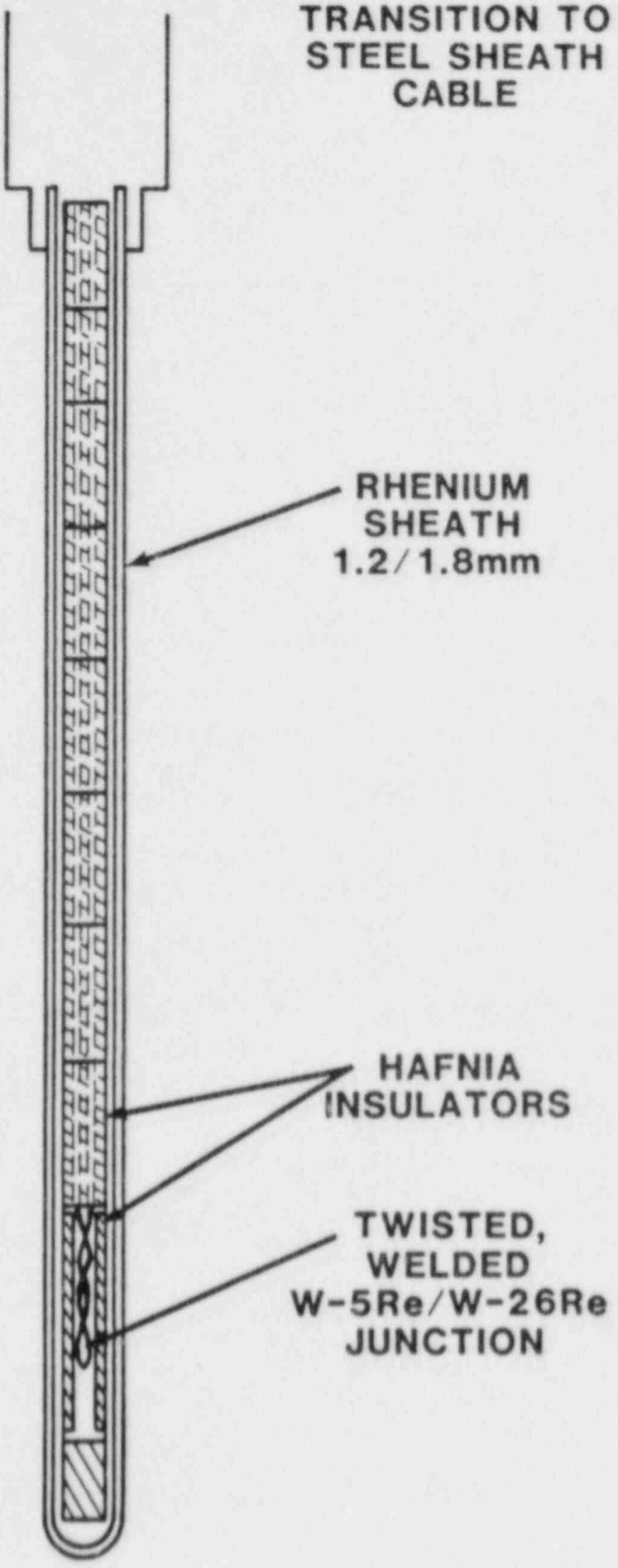

Figure 5. Thermocouple Detail

2.2.5.2 Ultrasonic Thermometers

UTs were developed at SNL for use in the D10 experiment. Early tests of the UT in 1982 and 1983 revealed significant measurement errors due to material transport at high temperatures, sensor wire stability in temperature gradients, and coil/remendur temperature effects. Material transport was reduced significantly by improvements in cleanliness and bakeout procedures. Sensor wire stability and remendur effects were improved by heat treatments and by using a new doped tungsten sensor wire. A prototype UT was tested in January 1984 with accuracy of ±50°C at 900°C and ±20°C at temperatures above 2000°C. A maximum test temperature of 2500°C was achieved. Details of UT development at SNL are reported in reference 15.

The D10 UT consisted of a doped tungsten sensor wire, a thoria insulator, and a rhenium sheath to protect the sensor wire from the sodium environment. Details of the sheathed portion of the sensor, which extended into the bed, are shown in Figure 6. The rhenium sheath was joined to a steel tube at a location well above the UO_2 bed. Each UT incorporated 14 sensing elements with notch spacings of 12 and 15 mm.

2.2.5.3 Experiment Instrumentation Locations

The bed was instrumented with 12 high-temperature rhenium-sheathed W/Re thermocouples, two sheathed UTs, and four 1.5-mm-diameter steel-sheathed K-type thermocouples. Additional steel-sheathed K-type thermocouples were used to measure sodium temperature, the temperatures of a 10-mm-thick SS 304 heat flux plate located below the crucible, and the temperatures of the containment structure, which were limited to 700°C as part of the experiment safety requirements.

A summary of instrumentation locations in the experiment is contained in Figure 7 and in Tables 1 and 2. The axial location listed in Table 2 refers to the center of each UT sensing element. Estimated position error for the thermocouples and UT elements is ±2 mm. The thermocouple error is largely due to the fact that the twisted wire junction was 5 mm long. This positional error has a potentially large influence on the interpretation of data in regions of steep temperature gradients.

The high-temperature thermocouples and the UTs penetrated the bed from above and were not bent due to the hard-fired hafnia insulation in the case of the thermocouples and the thoria and tungsten sensor wire in the case of the UTs. The K-type thermocouples were routed along the crucible wall and were bent into the bed at a constant elevation to the position indicated.

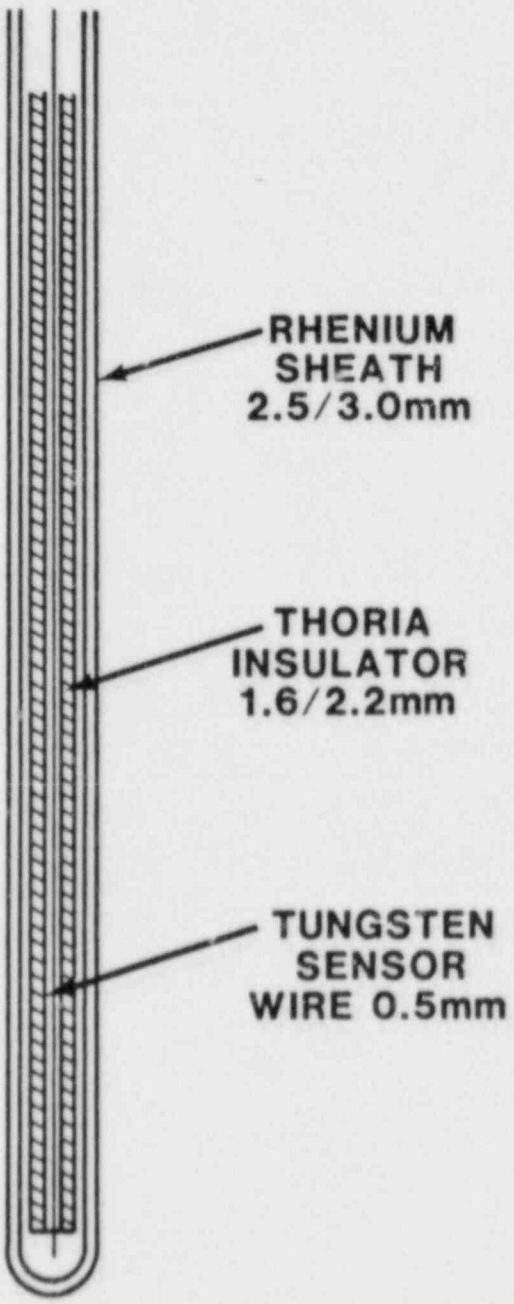

Figure 6. Ultrasonic Thermometer Detail

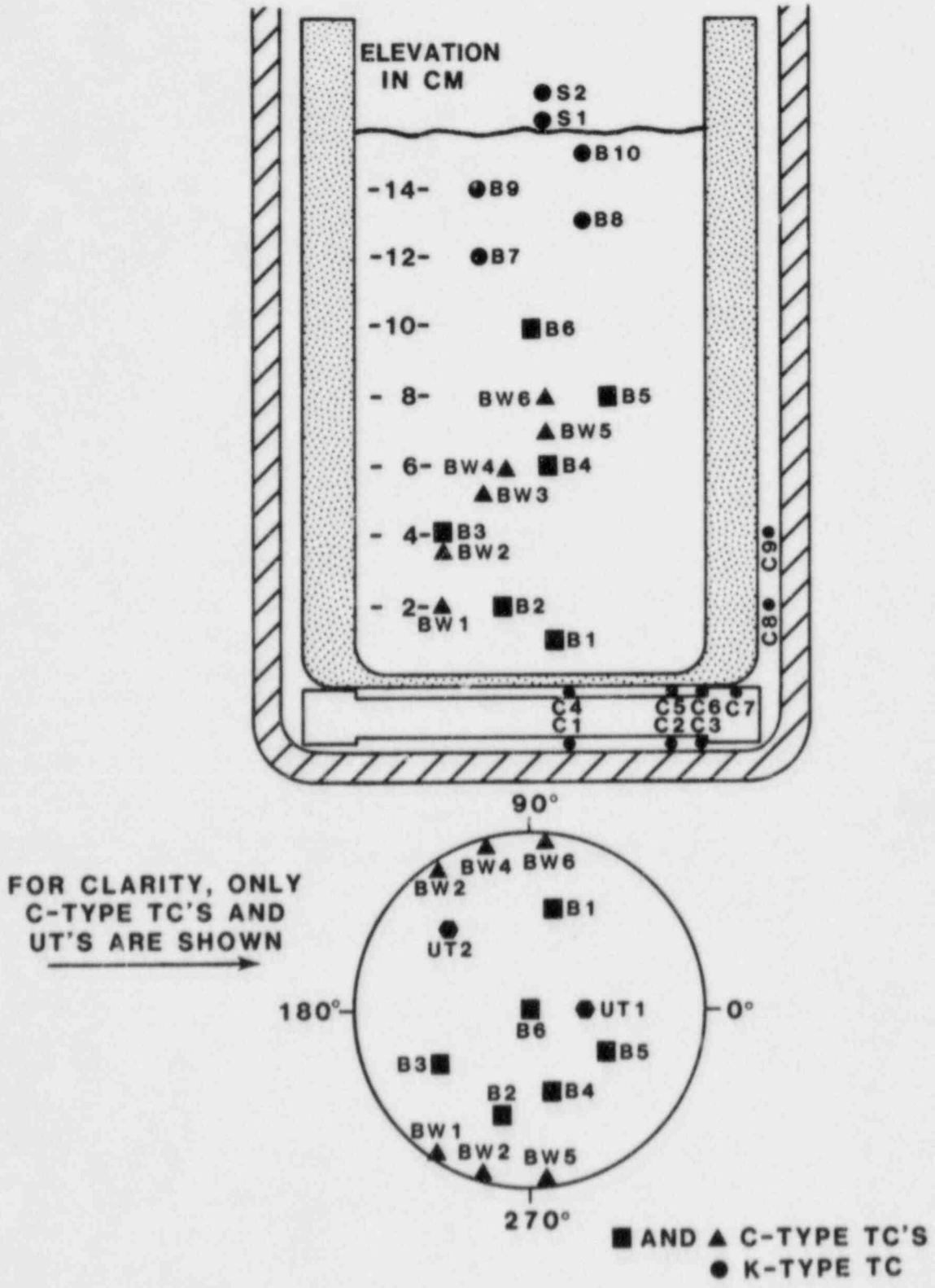

Figure 7. Instrumentation Layout

Table 1

Thermocouple Locations

Thermocouple	Radius (mm)	Z (mm)	θ
B1	30	13	65
B2	30	24	245
B3	30	43	210
B4	25	64	285
B5	25	82	330
B6	3	103	345
B7	16	120	105
B8	21	130	240
B9	28	140	305
B10	18	150	45
BW1	51	23	240
BW2	51	40	135
BW3	50	55	250
BW4	51	62	115
BW5	51	73	275
BW6	51	81	85
S1	4	161	80
S2	5	173	315
S3	10	205	100
S4	51	255	130
S5	60	550	-

Table 2

UT Notch Locations

Notch	Notch Length	Z (mm)
1	12	27
2	12	39
3	12	51
4	12	63
5	12	75
6	12	87
7	12	99
8	12	111
9	15	125
10	15	140
11	15	155
12	15	170
13	15	185
14	15	200

2.2.5.4 Pressure Transducers

Two Kaman Sciences KP-1911 pressure transducers were installed in both the primary and secondary containment vessels. These transducers performed a safety function of detecting leakage in either of the two containment barriers. Due to thermal gradients imposed on the transducers during the experiment, their accuracy was about ± 0.15 bar.

2.2.5.5 Data Acquisition System

The thermocouple data were sampled at 6- to 8-s intervals by an HP9845 minicomputer. The data were stored on disk by the HP9845 and were transmitted to an HP1000 for backup data storage and data display during the experiment. The UT data were recorded on about 1-min cycles by a second HP9845 and were stored on tape and transmitted to the HP1000 for display. The HP1000 provided data storage and merged the thermocouple and UT data into a file that could be utilized for real-time data display of any of the data channels. This display was essential to the conduct of the experiment, especially in the recognition of equilibrium conditions and incipient dryout.

2.2.6 Bed Characteristics

The D10 debris bed consisted of 8,143 g of fully enriched UO_2 particles with an approximately lognormal distribution ranging from 40 to 4000 μm (Figure 8). The effective particle diameter, calculated by the Fair-Hatch formula, is 173 μm. The UO_2, with an average density of 10.26 g/cm^3, formed a bed 16 cm high with a total volume of 1280 cm^3, giving a calculated open porosity of 38%.

The particles were prepared by Los Alamos National Laboratory by reduction of UO_3 in flowing hydrogen for 1 hr at 650°C followed by sintering for 1 hr in flowing helium and water vapor to obtain a ceramic-type UO_2 stable in air. The UO_2 was then pressed, crushed, sieve-sized, and fired in hydrogen at 1800°C for 24 hr. The fired particles were further crushed and sieve-sized to obtain the final particle distribution. The tendency for this UO_2 to adsorb water vapor was investigated at SNL (16). After 5 days in an 85% humidity environment, the UO_2 adsorbed approximately 0.015% water by weight. This water was easily desorbed within a few hours by heating to 100°C in vacuum.

As part of the experiment assembly in preparation for sodium filling, the primary containment, including the UO_2 debris, was baked out under vacuum for several hours. This bakeout was initiated by evacuating the sealed containment and purging twice with argon. The container was left connected to the cold trapped diffusion pump of a helium leak detector for a period of 16 hr at room temperature. It was then backfilled with argon to a pressure of 0.24 bar and heated to 300°C in a

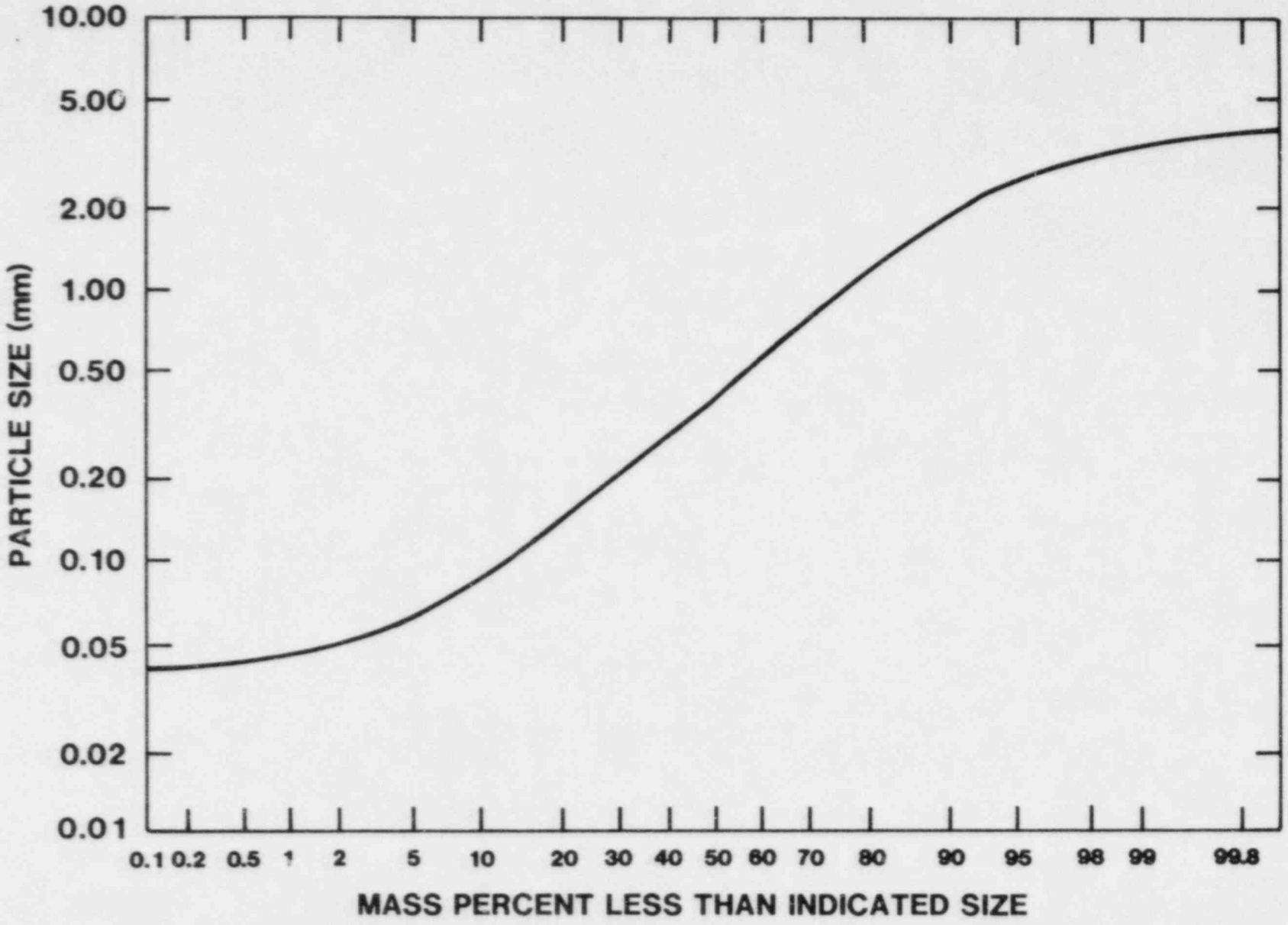

Figure 8. Particle Size Distribution

period of 4 hr. Twice during the heatup the containment was evacuated and purged with argon. The containment was then evacuated with the measured pressure at the inlet to the diffusion pump of 4×10^{-5} torr. After 3 hr at a temperature of 300°C, the pump inlet pressure had dropped to 1.6×10^{-5} torr and was decreasing at a rate of about 2%/hr. The bakeout was then terminated, and the experiment container was backfilled with less than 0.001-bar helium prior to filling with sodium. This helium pressure was provided to ensure that the debris contained a small amount of noncondensible gas so that a sodium superheat would be avoided during the initial heatup and approach to boiling during the experiment.

An x-ray of the bed and crucible was taken after sodium filling to ascertain the final bed height and the state of the bed surface. This x-ray revealed a bed height of 160 ± 2 mm, with no indication of significant erosion due to sodium filling (Figure 9).

2.2.7 Experiment Neutronics

Two-dimensional neutron transport calculations were performed with the TWOTRAN code to determine expected power profiles in the UO_2 debris (17). This calculation defined the bed with 8 equally spaced radial zones and 10 axial zones and used a 9-group cross section set tailored to the fast neutron spectrum that exists in debris bed experiments. Power peaking occurs at the radial boundary of the bed and at the top of the bed, with a maximum peak-to-average power ratio of about 1.1. A printout of the power distribution is included in Appendix B.

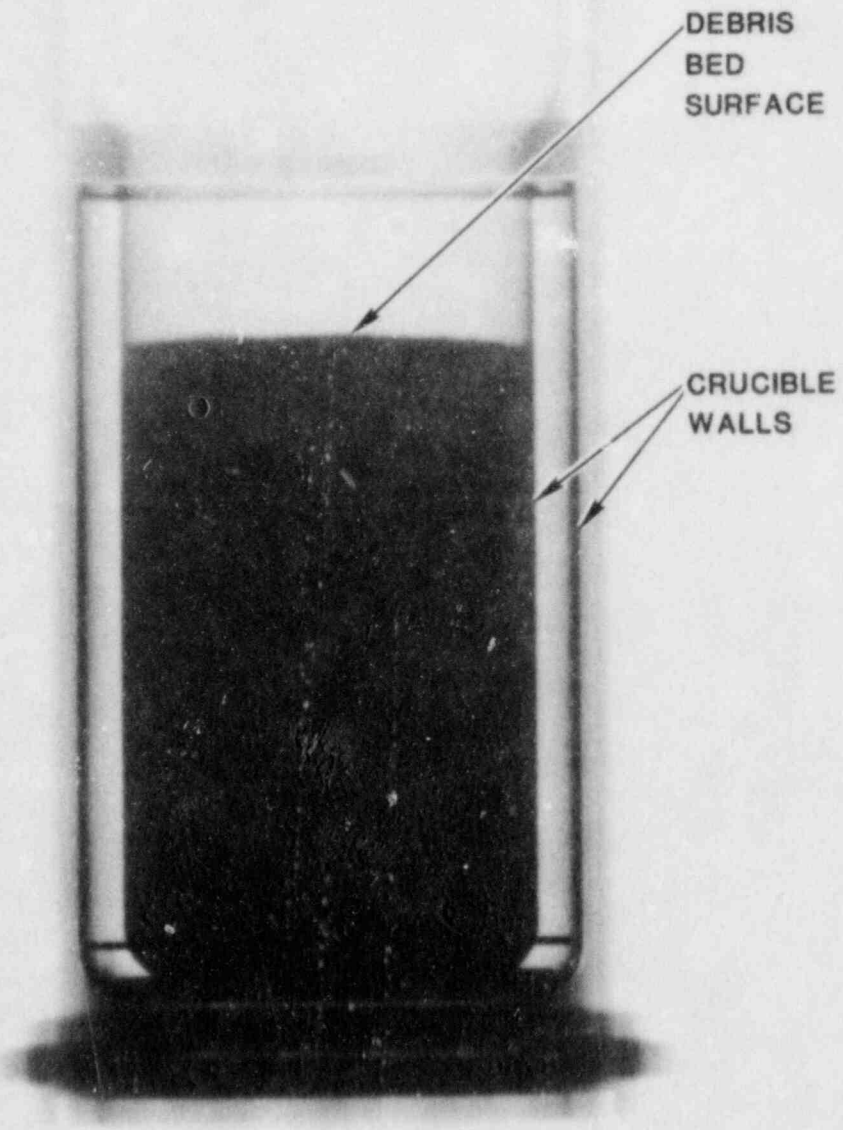

Figure 9. Pretest X-Ray

3.0 EXPERIMENTAL PROCEDURES AND RESULTS

The operating procedures to obtain most efficiently the desired data were proposed in December 1982 and were subsequently reviewed by program sponsors and SNL project staff prior to operation of the experiment. These procedures included conduction/convection investigations, two-phase heat removal and dryout, channel penetration, and channeled dryout investigations, all at various rates of downward heat removal. Finally, a dry zone was to be established and the power increased until a maximum temperature of 2500°C was achieved. This condition would be maintained for several hours, followed by an increase in downward heat removal. A copy of these procedures is shown in Appendix C.

3.1 Conduction/Convection Results

The experiment was begun on May 3, 1984 by melting the sodium, using the internal electrical heaters. After reaching a sodium temperature of 250°C, nuclear heating was initiated to begin the conduction investigations. The first control run was established at a sodium temperature of 350°C and an ACRR power of 90 kW to establish a reference temperature profile against which to make comparisons later in the experiment. A power calibration was then conducted by increasing ACRR power from 90 to 300 kW and observing the temperature rise (Figure 10). This calibration gave a power ratio of 1.77 W/g-MW_{ACRR}. From this point onward, recorded ACRR power levels were used to infer instantaneous debris bed power.

Sodium temperature was then increased to 600°C, and power was increased to achieve UO_2 temperatures of about 800°C, which were maintained for a period of 2 hr to ensure wetting of the UO_2 by the sodium. Various subcooled temperature profiles were then established in the bed at different sodium temperatures and rates of downward cooling. The experimental conditions during the conduction/convection investigations are summarized in Table 3. Z_a and $Z_{a,c}$ refer to the location of the adiabatic plane in the bed, determined from temperature profiles and calculated based on temperature measurements in the heat flux plate below the crucible (18). Temperature profiles, while providing the best means of identifying the adiabatic plane, can be used only when the bed is completely subcooled, which occurs only during the early portion of the experiment. For later experimental investigations, when boiling and dryout regions are present, the location of the adiabatic plane must be inferred based on a measurement of the downward heat removal. These calculations are significantly affected by the degree to which the experiment was allowed to equilibrate. Unsteady conditions can result in significant calculational errors.

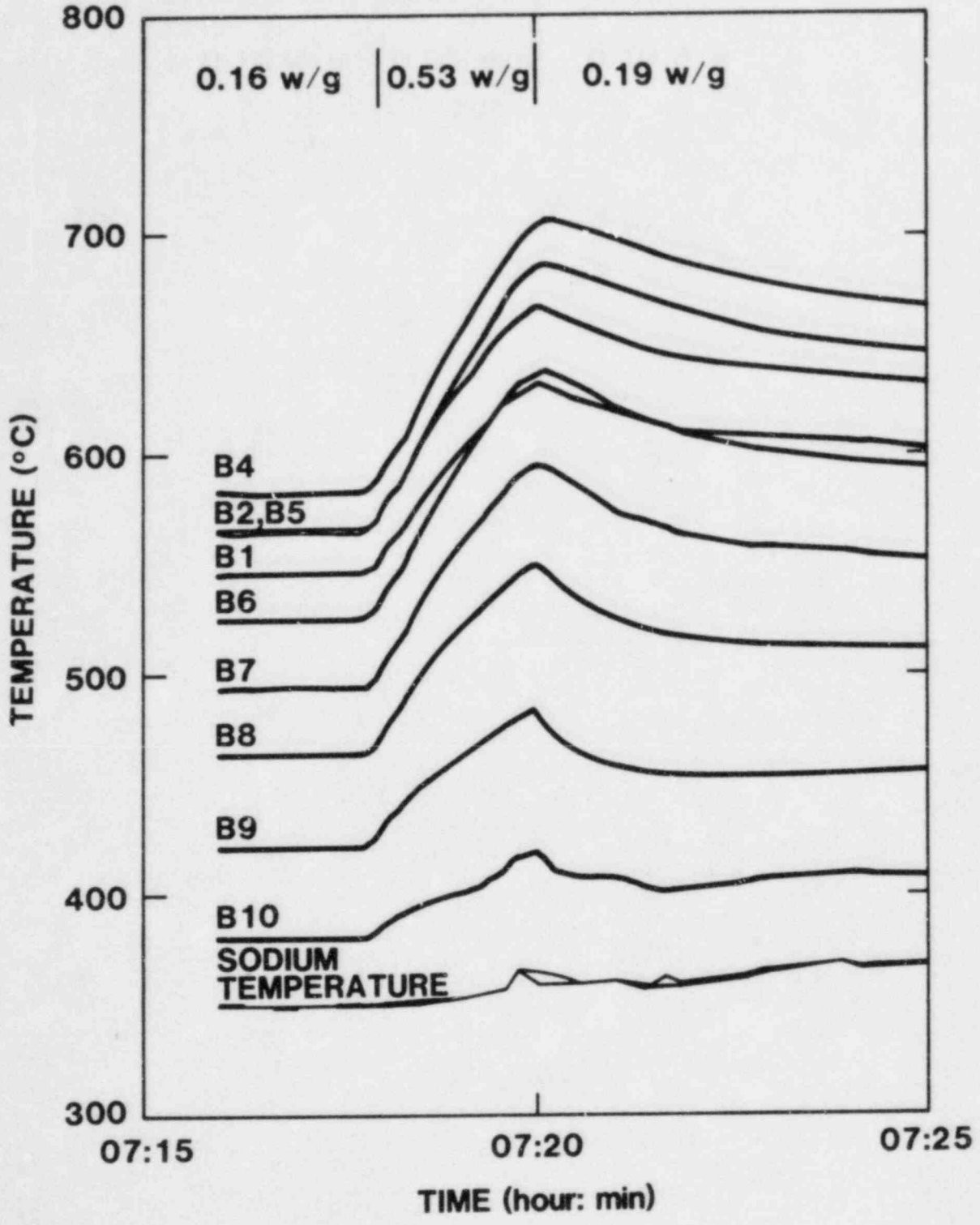

Figure 10. Power Calibration

Table 3

Conduction Investigations (May 3)

Time	Event	Bed Power (W/g)	He Flow (g/s)	Z_a (mm)	$Z_{a,c}$ (mm)	Sodium Temp (°C)	Max Bed Temp (°C)
0711	CR1	0.159	0	53	52	349	581
0718	PC1	0.531	0			360	704
0853	CR2	0.212	1	79	84	595	788
1023	CR3	0.159	0	62	63	595	810
1219	CR4	0.159	2.5	98	103	596	677
1340	CR5	0.159	6.4	115	116	607	643
1440	CR6	0.159	11.7	97	97	356	434
1623	CR7	0.159	0	62	59	350	549
1624	PC2	0.531	0			350	700
1724	CR8	0.248	0	56	47	355	753
1754	CR9	0.319	0	55	40	352	849

CR = Control or conduction run
PC = Power calibration

Temperature profiles during these first investigations were compared with two-dimensional calculations made using the Kampf-Karsten conductivity for the bed. The calculations were consistent with the observed data, indicating that the assumed conductivity was appropriate.

An evaluation of temperatures at the bottom of the bed revealed a higher temperature drop across the bottom of the crucible than one would expect if the liquid tin were in perfect thermal contact with the Ta-10W walls. Temperature drops of 40 to 90 degrees were observed, about twice what would be calculated for the tin-Ta-10W layers. Although uncertainty in the location of thermocouple junctions could account for part of this discrepancy, a likely explanation is that the tin did not wet the Ta-10W completely, even though interface temperatures of 750°C were attained. Such a partially wetted surface would provide some increase in contact resistance between the metallic layers.

3.2 Two-Phase Heat Removal and Dryout

At a sodium temperature of 350°C and downward heat removal of about 80 kW/m^2, power was gradually increased until boiling was observed in the bed at a power of 0.345 W/g. The onset of boiling is indicated in Figure 11 by thermocouples B3, located at an elevation of 43 mm, B4 (64 mm), and BW3 (55 mm) as a characteristic leveling off in temperature while at constant

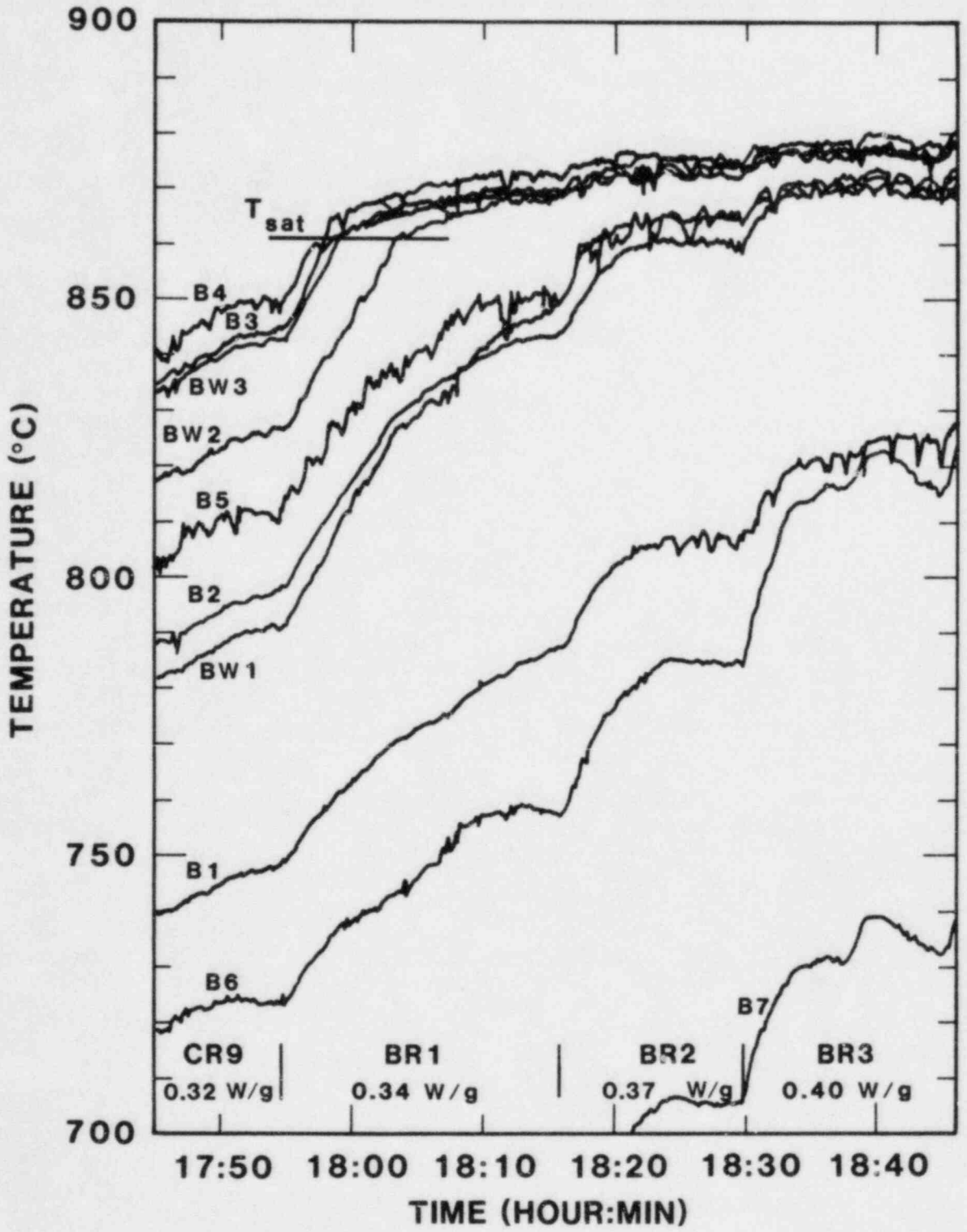

Figure 11. Onset of Boiling

power. Additionally, the temperature gradient in the bed is reduced because of boiling heat transfer, as indicated by thermocouples above and below the boiling region, which continue to increase in temperature. Three steady-state boiling runs with temperatures near the saturation temperature of 861°C are shown in Figure 11. The saturation temperature is calculated to increase because of expulsion of liquid from the bed, which compresses the experiment cover gas. This increase is determined to be $0.63\ L$, where L is the thickness of the boiling zone in centimeters. The observed temperatures in excess of nominal saturation are due to capillary force induced by the vapor in the boiling zone. The local boiling temperature reflects the local pressure in the vapor.

Bed conditions at various times are shown in Table 4. During the three boiling runs, the calculated adiabatic plane indicates that all heat generated below 40 mm is transported downward. Figure 11 shows that thermocouple B2 (24 mm), located below the adiabatic plane, indicates boiling at a later time than B3 (43 mm), located very near the adiabatic plane. This indication of downward heat transfer by boiling is confirmation of the downward boiling observed out-of-pile in inductively heated steel-water beds by Barleon, Thomauske, and Werle (19).

Table 4

Boiling and Packed Bed Dryout

Time	Event	Bed Power (W/g)	He Flow (g/s)	$Z_{a,c}$ (mm)	Sodium Temp (°C)	Max Bed Temp (°C)
1815	BR1	0.345	0	40	349	872
1829	BR2	0.372	0	38	355	876
1845	BR3	0.398	0	41	352	878
1900	IPD1	0.425	0	43	350	947
1910	EPD1	0.451	0	43	360	1163
2022	IPD2	0.478	2.5		352	1109
2127	IPD3	0.584	12.2		349	989
2152	IPD4	0.478	0		343	927

BR = Boiling run
IPD = Incipient packed bed dryout
EPD = Extended packed bed dryout

As power was increased further, dryout was observed in the bed at a power of 0.425 W/g. Temperatures in the bed during this first dryout are shown in Figure 12. It appears that the dryout began at an elevation between 55 and 60 mm, since BW3,

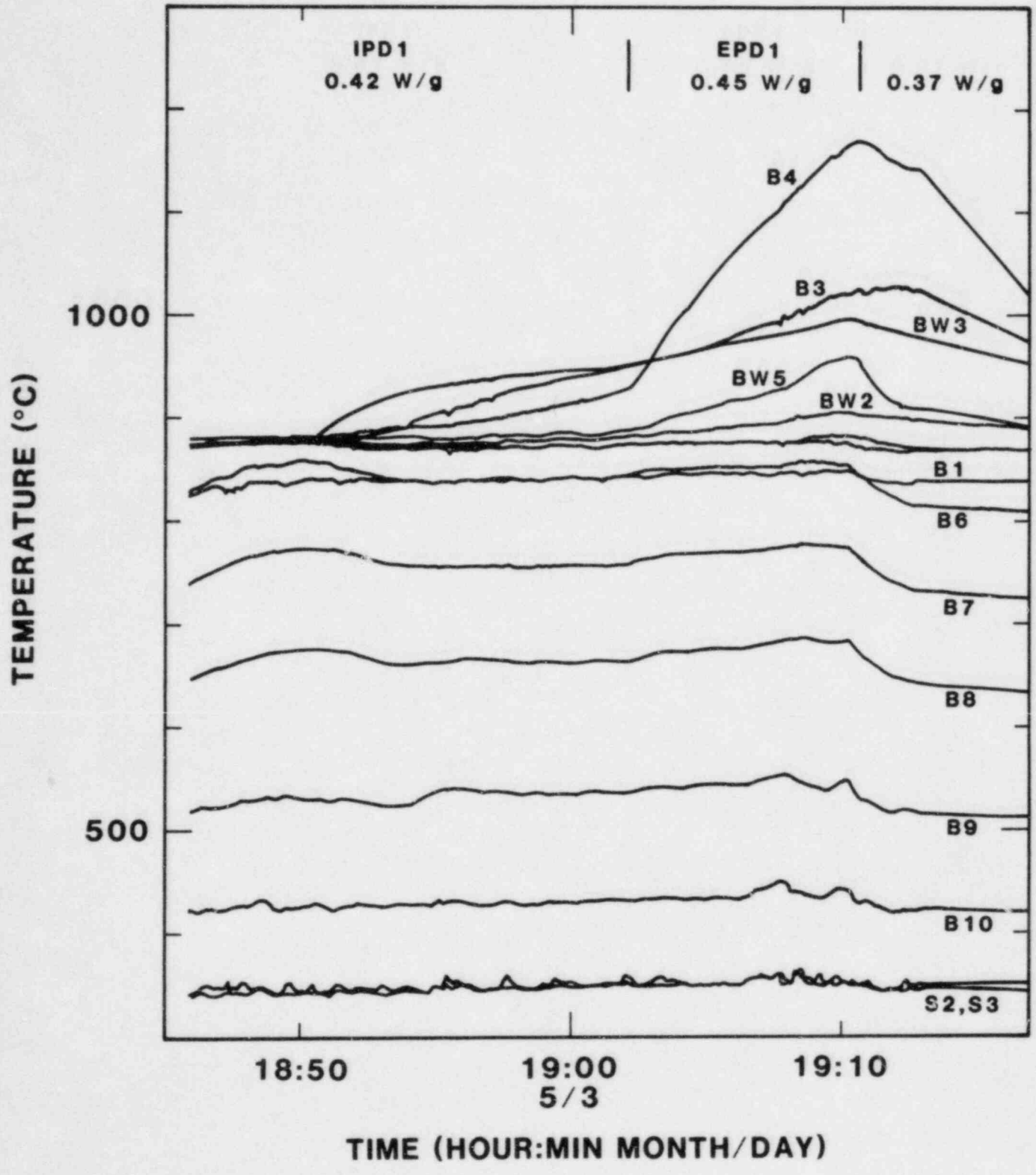

Figure 12. Packed Bed Dryout

located at 55 mm, first shows an indication of dryout. B3 (43 mm) and B4 (64 mm) began increasing in temperature within 1 min after BW3. The response of B4 to the power increase at 1902 would indicate that it is nearer to the center of the dry zone than B3. The location of the adiabatic plane at the onset of dryout is inferred to be near 55 mm. Calculated locations based on the heat flux plate remain nearly constant during the onset of boiling and dryout (Tables 3 and 4). The last well-characterized location of the adiabatic plane was made using temperature profiles during CR8 and CR9 and was at 55 mm. This location is supported by the indications of B1 (13 mm) and B6 (103 mm), which are at nearly identical temperatures, suggesting that the adiabatic plane is near 58 mm.

The dry zone appears to extend completely across the crucible, as indicated by the temperature increase of BW2 (40 mm) and BW3 (55 mm), which are located on opposite sides of the crucible. The growth of the dry zone completely across the crucible was felt to be important to establish a one-dimensional condition in the bed. This expansion of the dry zone would eliminate the possibility of liquid flow around the dry zone, which could replenish liquid in the lower subcooled zone.

The dryout was repeated at higher rates of downward cooling (Table 4). The measured incipient boiling power of 0.345 W/g compares with a calculated value using the Lipinski model of 0.32 W/g while the incipient dryout power was 0.425 W/g compared to a calculated value of 0.35 W/g (20).

3.3 Channel Penetration Investigations

Following the initial dryout investigations, the power required to induce channeling in the bed was determined by increasing power from 0.425 W/g to 0.63, 0.85, and finally 1.06 W/g with a requenching of the dry zone that had formed following each power step by a power reduction back to 0.425 W/g (Table 5).

Table 5

Channel Penetration

Time	Event	Bed Power (W/g)	He Flow (g/s)	$Z_{a,c}$ (mm)	Sodium Temp (°C)	Max Bed Temp (°C)
2256	EPD2	0.63	0	--	360	1219
2322	EPD3	0.85	0	--	362	1138
2336	CF1	1.06	0	--	351	871

CF = Channel formation

At 0.63 and 0.85 W/g, a packed bed dry zone was present at the time the power was increased and grew until temperatures reached about 1200°C. This growth of the dry zone indicated that channeling did not occur at these power levels. At a power of 1.06 W/g, a dry zone was not initially present and did not form (Figure 13). Rather, the boiling temperature increased as local pressure in the bed built up and then suddenly was released.

The temperatures in the boiling zone were used to infer the local pressure of the vapor at the time of channel penetration (Figure 14). Also shown is the local pressure due to the weight of the submerged bed. The vapor pressure in the boiling zone was well over that required to move particles in a frictionless and loose bed. The peak overpressure of 0.35 bar occurred at an elevation of 64 mm and was about 7 times the overpressure due to the weight of the bed of 0.05 bar at that elevation. This implies a "sticking factor" that inhibits channel formation in a subcooled bed. It is not known how the sticking factor depends on subcooled zone thickness and aspect ratio, particle roughness, or bed porosity. However, because of the large overpressure required to move the particles, when the event finally occurred, it was disruptive. The disruption was aided by the vaporization of liquid sodium in the boiling zone, which was superheated at the time by about 40°C relative to the saturation temperature following the event.

3.4 Channeled Dryout

Following the disruptive event described above, power was reduced to 0.32 W/g and then increased in steps to a maximum of 0.85 W/g. It did not appear that a dry zone was present at this power. The dryout power for a packed bed with suppressed channels as a function of bed porosity is calculated using the Lipinski Debris code (Figure 15) (18). The upper curve assumes a constant bed height of 16 cm while the lower curve more realistically assumes an increased bed height consistent with the change in porosity. X-rays of the D10 bed taken after the experiment (Figure 16) revealed that the bed height had increased slightly during the experiment, to 167 ± 3 mm. This corresponds to an increase in average porosity from 0.38 to 0.40, although the porosity in the upper portion of the bed undoubtedly increased to a greater extent than the lower portion. Even so, a porosity greater than about 0.45 in the upper bed is unlikely, which should not increase dryout power significantly. In addition, calculations of bed porosity following the disruption event using power calibration data would indicate that the porosity had increased slightly, to about 0.41 (16).

The dryout calculations (Figure 15) would indicate that the observed lack of dryout at 0.85 W/g would require a packed bed with a porosity of 0.6 to 0.65 (bed height of 250 mm). This is not consistent with the observations made with respect to

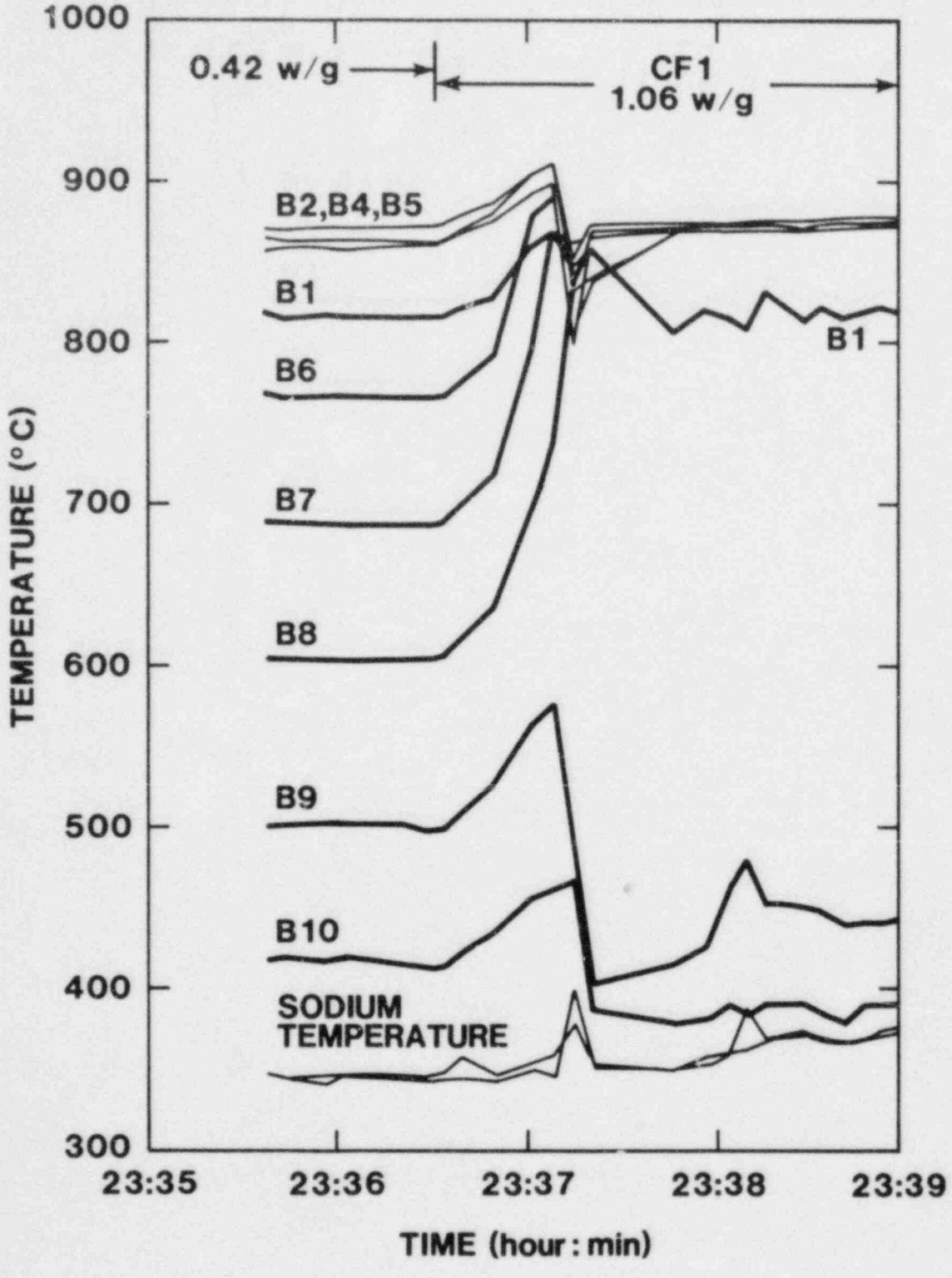

Figure 13. Channel Penetration

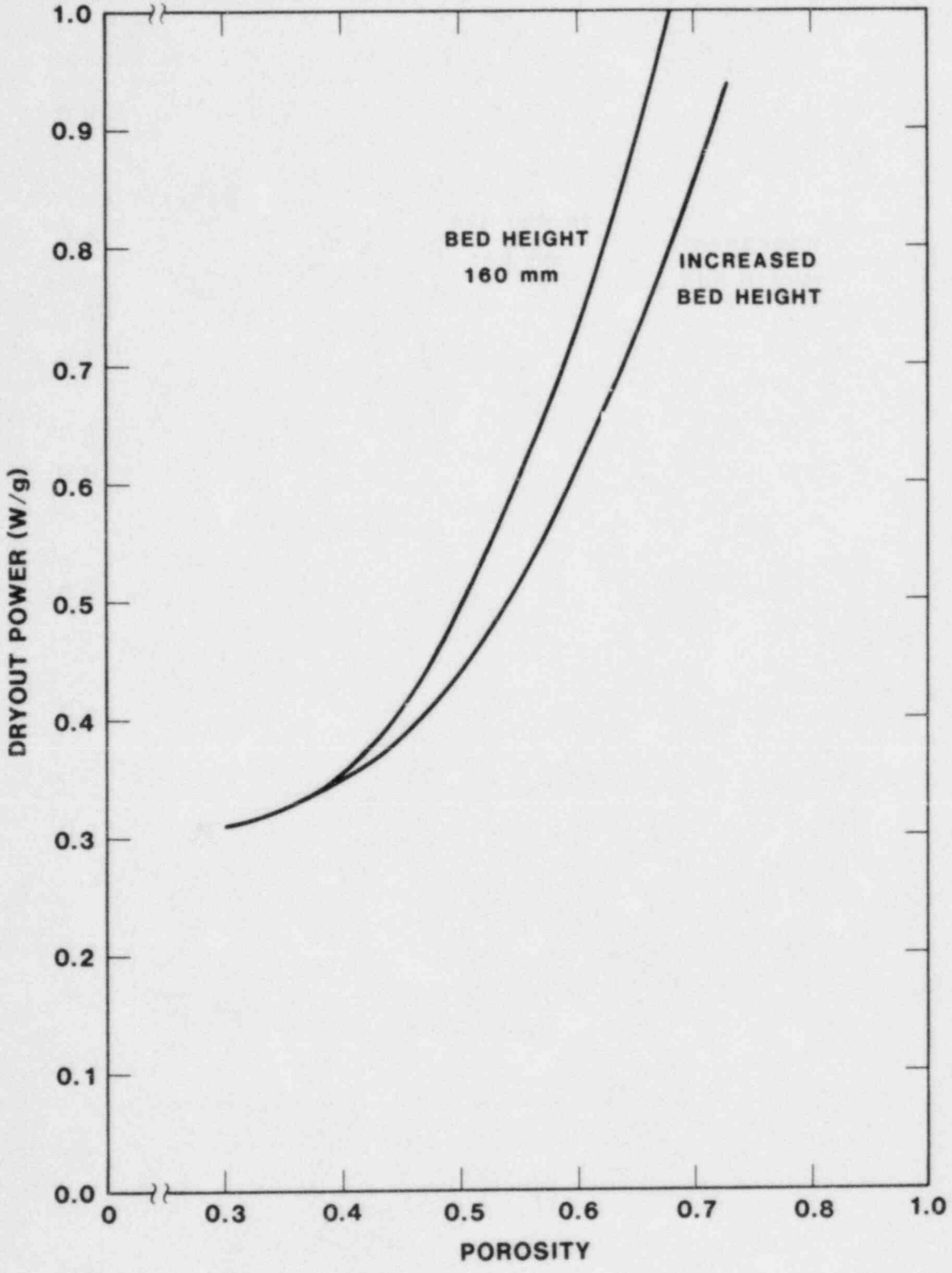

Figure 14. Bed Pressure prior to Channeling

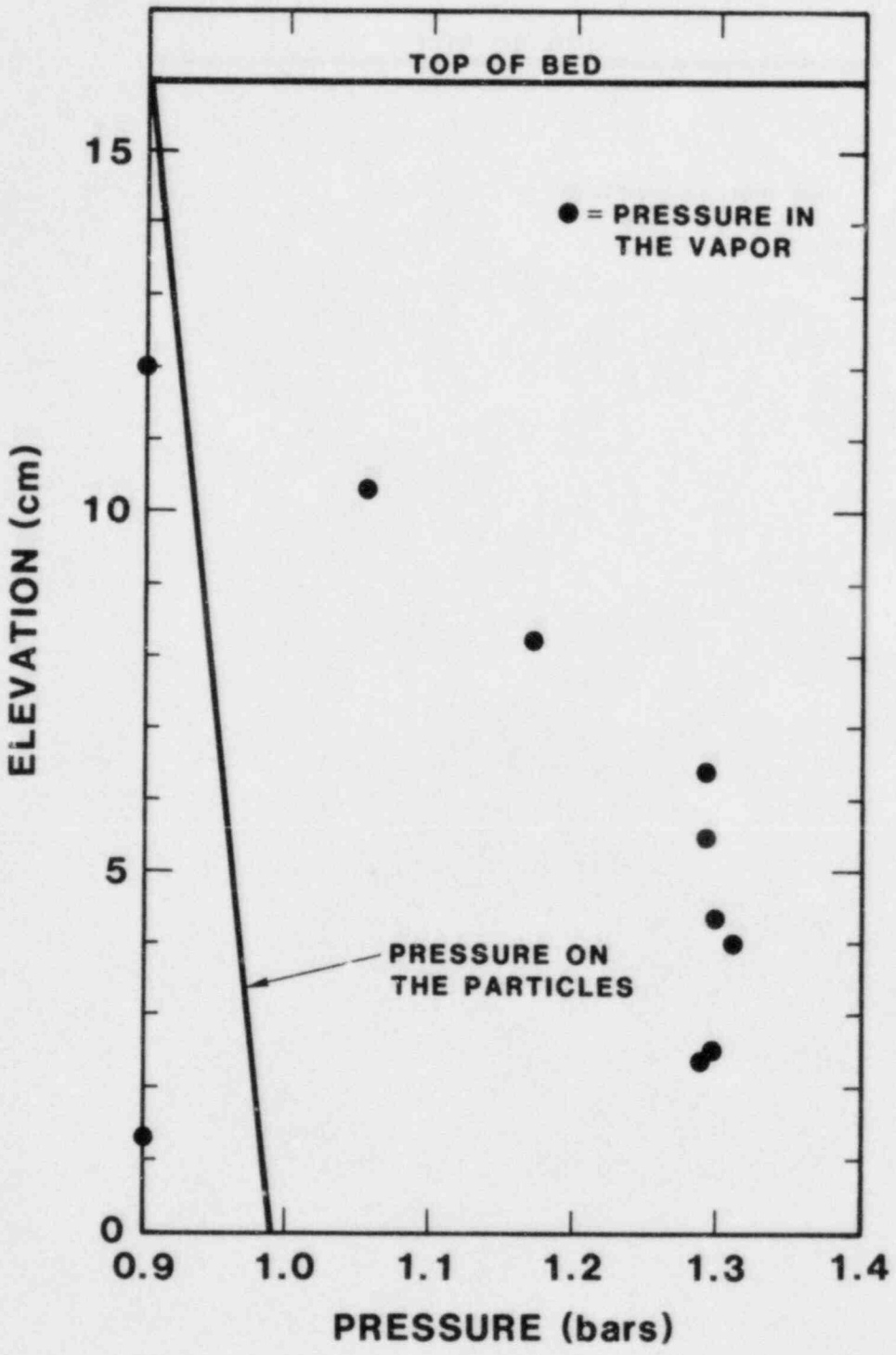

Figure 15. Calculated Packed Bed Dryout

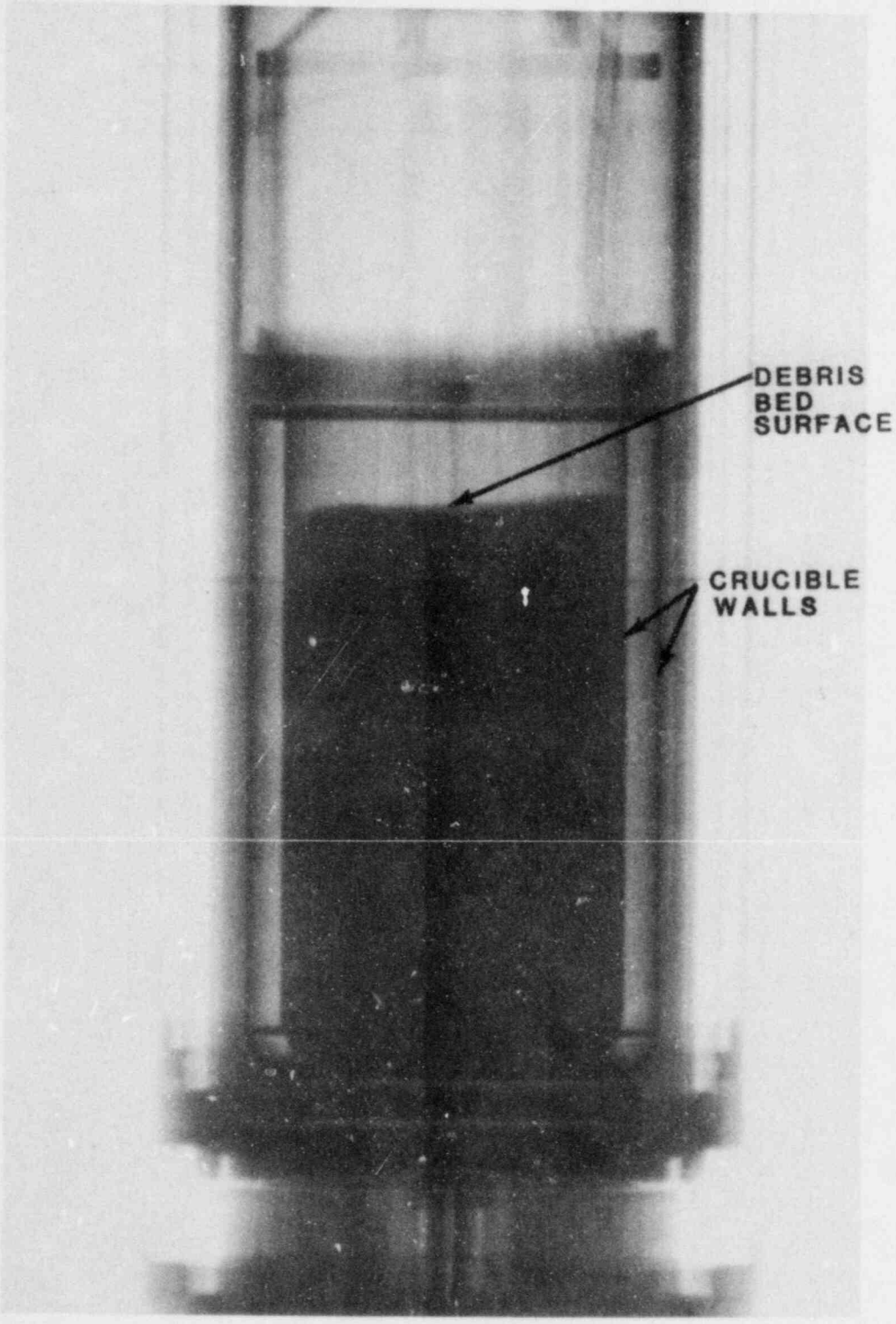

Figure 16. Posttest X-Ray

porosity, and it is concluded that even though the bed may have been more porous, channeling did occur in the bed at a power of about 1 W/g and channels remained in the bed after the disruption event.

Power was then decreased and the size of the boiling zone was allowed to shrink in an attempt to reestablish a packed bed state. Two stable states were established with small boiling zones. Power was then increased until dryout was observed at a sodium temperature of 540°C and a power of 1.06 W/g, indicating that the bed was permanently channeled and that the event had increased the coolability (i.e., dryout power) by a factor of 2.5. The dry zone extended across the crucible, as BW2, BW3, and B2 all indicated temperatures above the saturation temperature.

Additional channeled dryouts were established with larger downward heat removal. These data are summarized in Table 6.

Table 6

Channeled Dryout (May 4)

Time	Event	Bed Power (W/g)	He Flow (g/s)	$Z_{a,c}$ (mm)	Sodium Temp (°C)	Max Bed Temp (°C)
0026	BR4	0.345	0	--	355	862
0204	BR5	0.319	0	--	351	860
0303	ICD1	1.06	1.6	--	540	918
0604	ICD2	1.24	2.6	--	640	988
0635	ICD3	1.42	1.8	--	602	1024
0802	ICD4	1.50	14.0	--	620	972

ICD = Incipient channeled bed dryout

The power required to produce dryout and the growth of the dry zone in the channeled state as power was increased do not agree with the Lipinski model (18). This model yielded dryout powers for a channeled bed of about 3.0 W/g and very thin dry zones of about 6 mm at 3.5 W/g. These calculations are in contrast to the 30-mm dry zones that were observed during the incipient dryout investigations at a power of 1.42 W/g.

3.5 High-Temperature Dryout

A large dry zone in the channeled bed was established by increasing power from 1.06 W/g to 1.77 W/g initially. A thick dry zone was established rather quickly, as evidenced by the

immediate onset of dryout at BW2 at 40 mm, BW3 at 55 mm, and BW5 at 73 mm, after the increase in power (Figure 17). The dry zone expanded to BW1 at 23 mm and B2 at 27 mm within 2 min after the power change, to B1 at 13 mm after 5 min, and to B4 at 64 mm after about 9 min. Several power adjustments were required to maintain temperatures below previously established safety limits. The power reductions quenched the dryout at 64 mm in the center of the bed and nearly so at 73 mm on the wall of the crucible. The dry zone was stabilized at a power of 1.5 W/g, which was maintained for 70 min. Maximum measured temperature in the bed was 2060°C at that time. A peak measured temperature of 2240°C was observed during the power adjustments.

A distinction must be made between measured temperatures and actual debris temperatures. Three-dimensional heat transfer calculations were made prior to the experiment to determine the effect of instrumentation on bed temperatures and to relate measured temperatures to debris temperatures at locations not in proximity to the instrumentation. These calculations indicated that the thermocouples would indicate temperatures less than the maximum bed temperatures because of heat transfer along the highly conductive sheath and because of the radial temperature gradient. For the thermocouples, located at radii of 25 and 30 mm, this gradient could result in a temperature drop of several hundred degrees (21). For the purposes of discussion and for this preliminary interpretation of bed behavior, reference will be made to measured temperatures. Although additional three-dimensional calculations will be required to establish reliable estimates of the maximum debris temperatures achieved in the experiment, the pretest calculations that were accomplished would indicate that debris temperatures in excess of 2500°C were achieved.

Power was then increased slightly, to 1.59 W/g, since temperatures were below maximum limits. This power was maintained for an additional 65 min, at which time the maximum temperature was 2186°C. Downward cooling at this time was about 360 kW/m^2. Bed behavior during the high-temperature operation appeared quite stable and did not vary with time.

The power was then reduced to the incipient dryout power of 1.24 W/g with downward cooling of about 280 kW/m^2. The dry zone did not quench at this power, rather it was reduced slightly in extent with a maximum measured temperature of 1864°C. An additional power reduction to 1.06 W/g reduced the extent of the dry zone only slightly, with a maximum temperature of 1666°C. A power reduction to 0.71 W/g rapidly quenched the dry zone 3 hr 15 min after the onset of dryout. The bed temperatures during this period are shown in Figure 17.

The behavior of thermocouple B1 is due to the junction being below the location of maximum temperature of the sheath (near

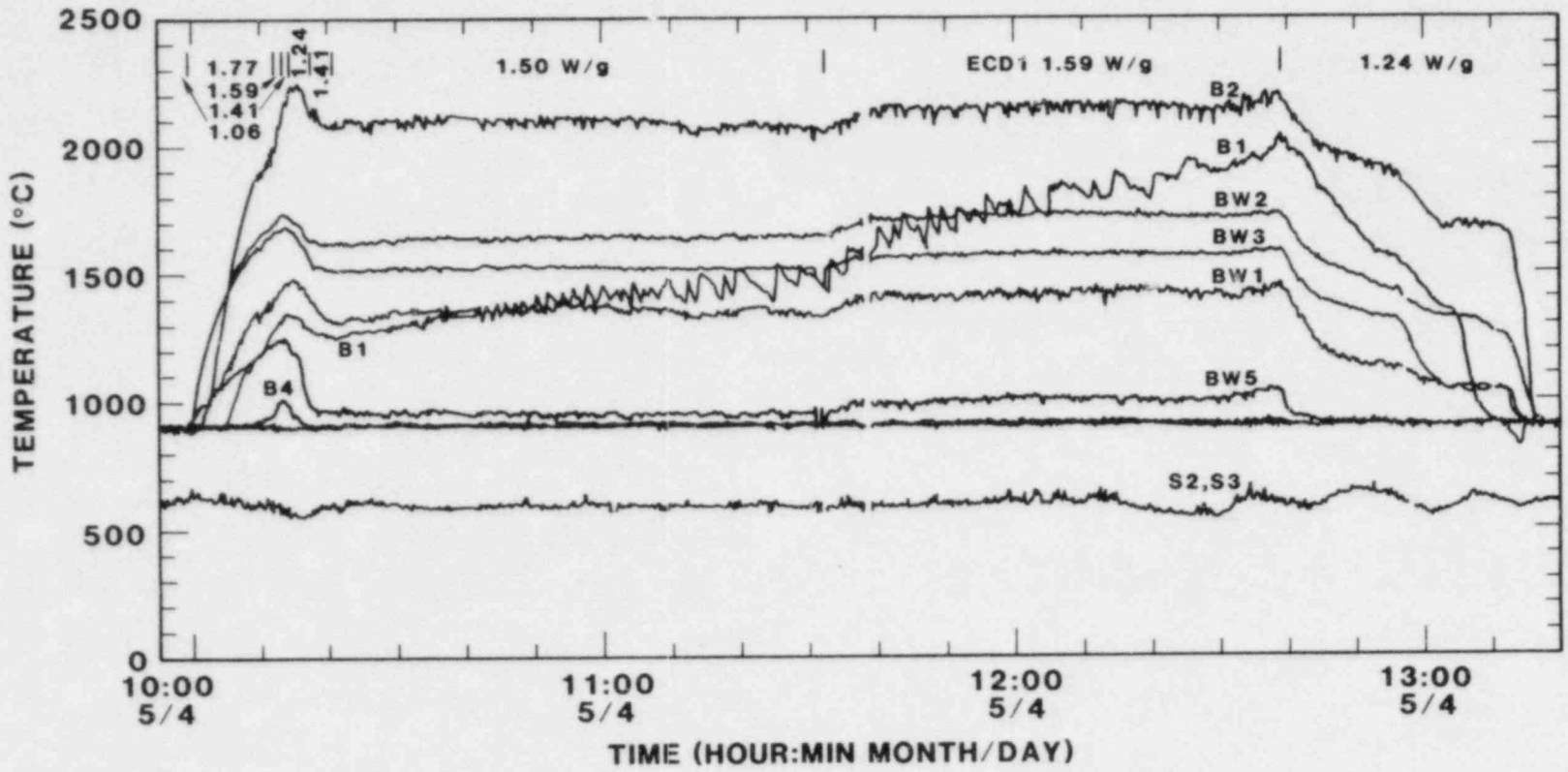

Figure 17. High-Temperature Dryout

40 mm). At temperatures above 1600°C, the HfO_2 insulation becomes conductive and a shunting occurs, which causes an electromagnetic force (emf) corresponding to the peak temperature to be measured. This shunting occurred gradually over a period of 2 hr. Thermocouple B2, even though its junction is located at an elevation of 27 mm, probably measures a temperature very close to the maximum sheath temperature because of heat transfer along the sheath. This is supported by the fact that the temperature does not vary with time, as did B1. Thus, B2, located at a radius of 30 mm, should be quite useful in estimating peak debris temperatures.

The UT data, although not as accurate as the thermocouple data, provide valuable information about the temperature profile in the dry zone (Figure 18). The stability of the data indicates that the UTs are functioning well throughout the dryout. The stable temperature profiles at a power of 1.59 W/g are plotted in Figure 19. These profiles indicate that the adiabatic plane in the dry zone is slightly above 40 mm. A location of 36 mm is calculated based on data from the heat flux plate. The signals from the lower two notches of UT1 were not useful in providing data during this first dryout. They later became functional and were useful in the last high-temperature dryout established on May 8.

The temperature below the crucible was then decreased 150°C by increasing helium flow, and the power was increased to 1.42 W/g and eventually 1.68 W/g to reestablish a high-temperature dryout. In this dryout (Figure 20), the dry zone extends to 64 mm in the center of the bed, as evidenced by B4, and to 73 mm at the crucible wall (BW5). Heat flux calculations indicate that the adiabatic plane has moved upward about 5 mm as compared to the first high-temperature dryout. The dryout was nearly quenched by a power reduction to 1.24 W/g; however, a dry zone appeared to remain, as evidenced by BW2 and BW3.

The events recorded during the high-temperature operations are summarized in Table 7.

These investigations concluded the first period of operation of the experiment, all planned areas having been successfully investigated.

3.6 Additional Experiment Operations

Reviewing the experimental data accumulated during the first period of experiment operation, it was concluded that the most significant event that had occurred was the formation of channels, which significantly increased the coolability of the bed and which appeared not to be reversible, as was the case during the D9 experiment (5). Further experiment operation appeared to be useful in providing additional data if the bed

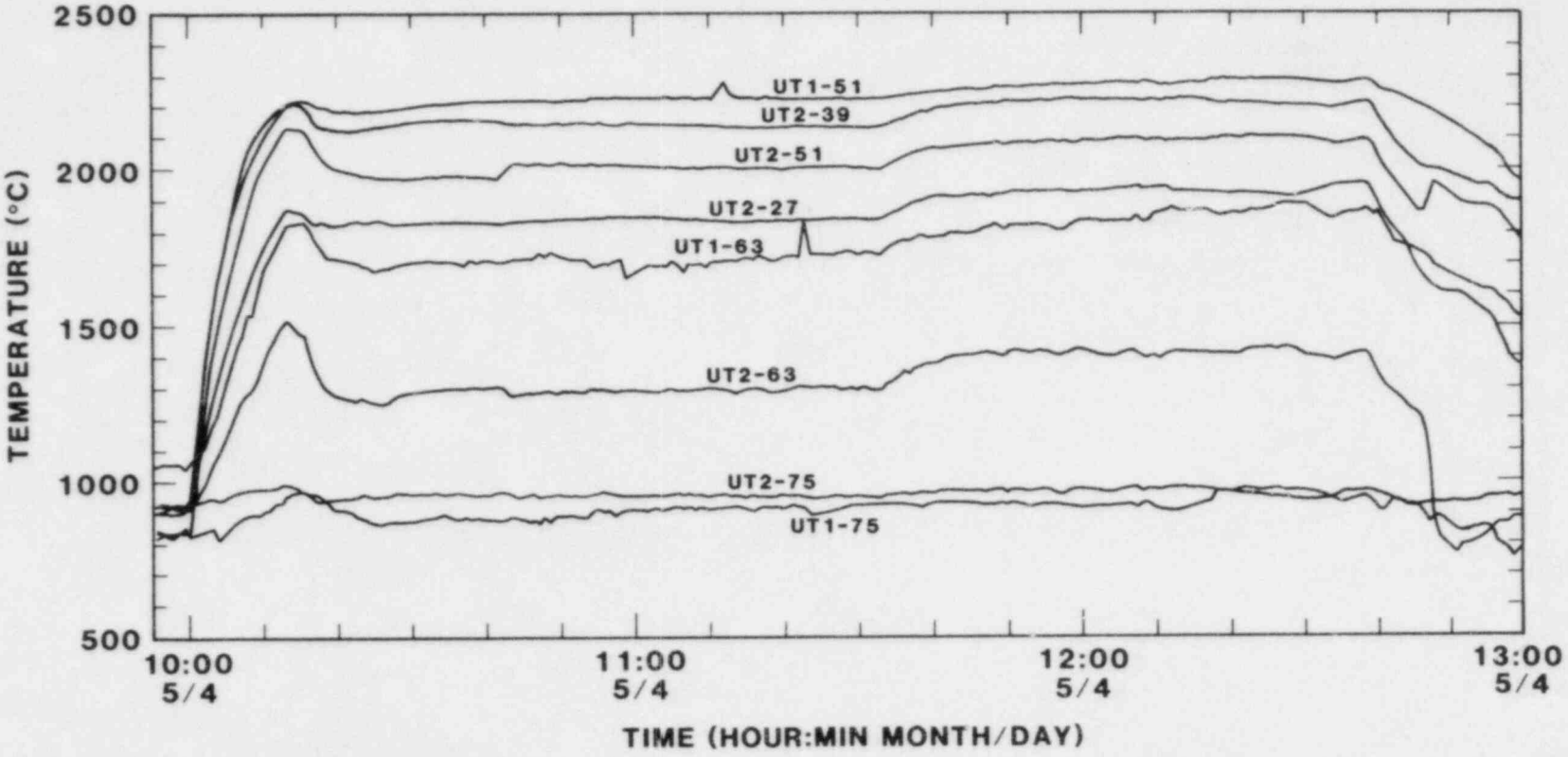

Figure 18. UT Data during High-Temperature Dryout

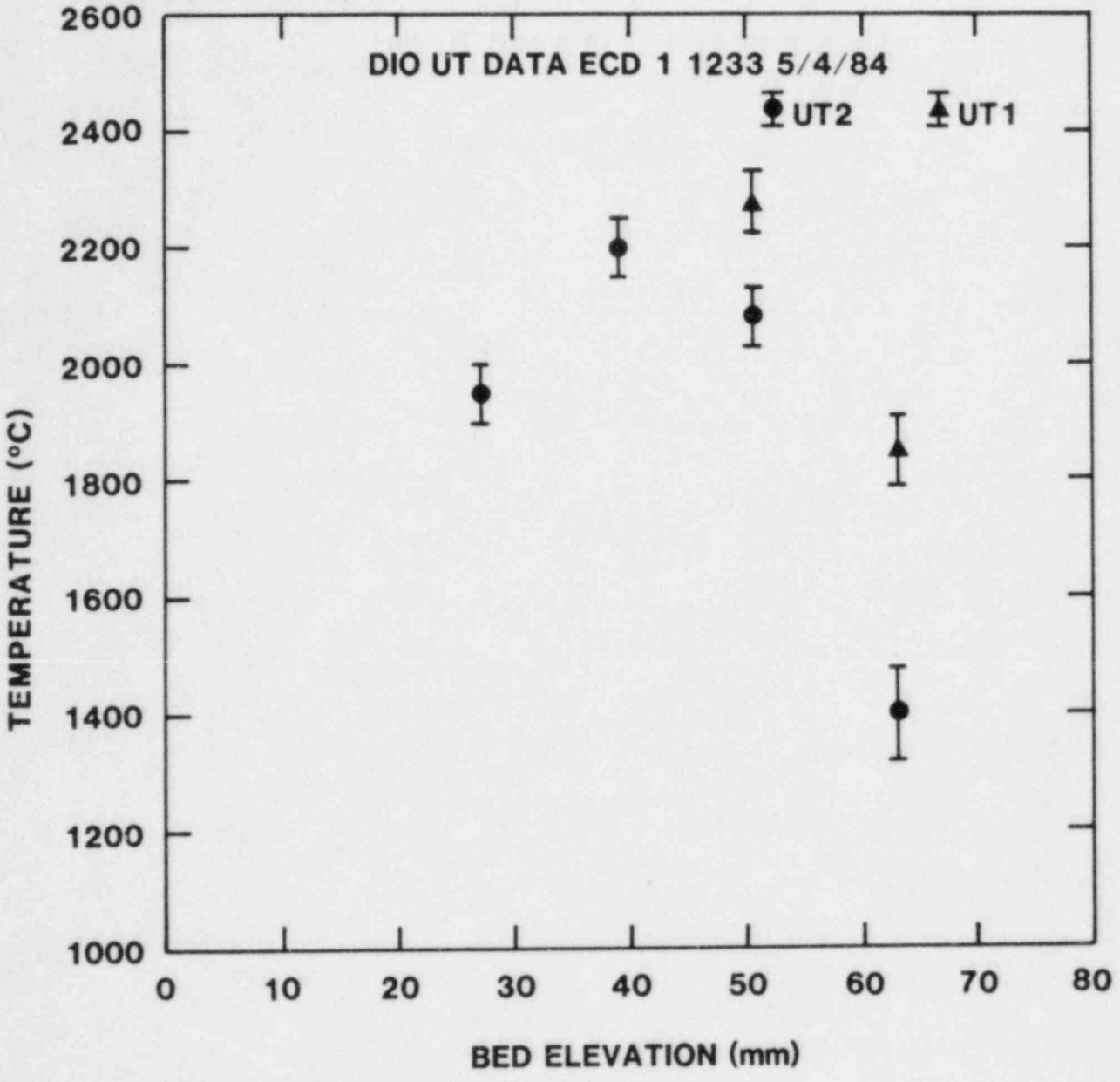

Figure 19. UT Data at the End of ECD1

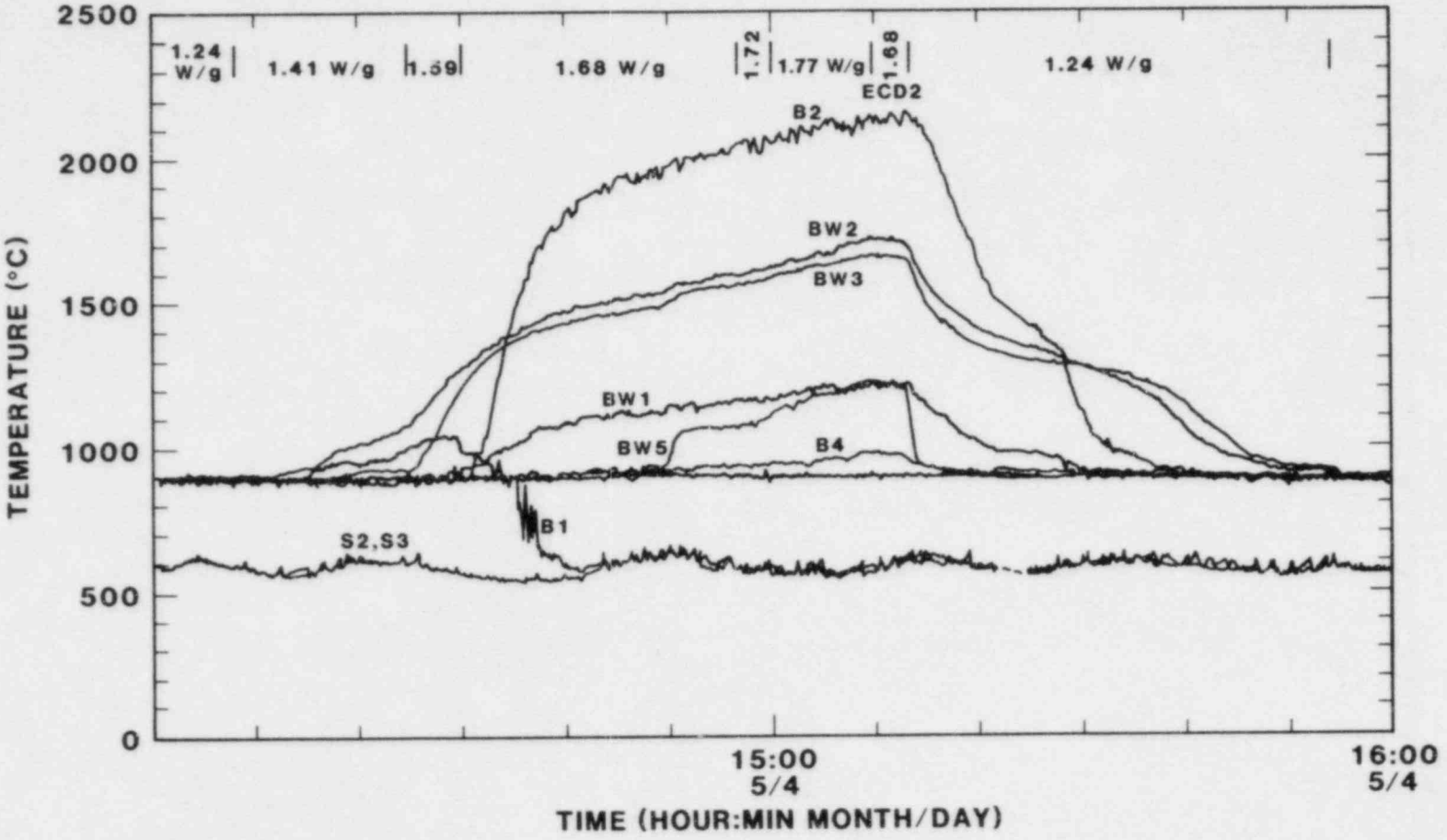

Figure 20. ECD2 High-Temperature Dryout

Table 7

High-Temperature Investigations

Time	Event	Bed Power (W/g)	He Flow (g/s)	$Z_{a,c}$ (mm)	Sodium Temp (°C)	Max Bed Temp (°C)
1237	ECD1	1.59	5.0	36	600	2186
1255	Q1	1.24	3.5		617	1864
1311	Q2	1.06	2.3		603	1666
1318	Q3	0.89	1.4		597	907
1423	ICD5	1.42	7.6		620	1067
1512	ECD2	1.68	9.1	41	600	2126
1554	Q4	1.24	6.2		601	923
1722	CR10	0.159	0		354	597
1726	PC3	0.531	0		353	714

ECD = Extended channeled bed dryout
Q = Quench

could be returned to a packed state. An operational procedure using superheat disturbances was devised to attempt this (Appendix C).

The experiment was restarted and superheat disturbances as high as 45°C were induced in the bed. The bed appeared to remain channeled, so a power step from 0.159 to 1.77 W/g was made with the bed initially in a subcooled state in an attempt to disrupt and repack the bed. This was also unsuccessful. Another superheat of 32°C was induced, again with no apparent change in bed characteristics.

Three stable high-temperature dry zones at maximum downward cooling were then established to study postdryout conditions in a channeled bed (Figure 21). A maximum temperature of 1909°C was measured at B2 at a power of 1.77 W/g. The UT data, including the lower two notches of UT1, during the high-temperature operation are shown in Figures 22 and 23. These data indicate that the adiabatic plane during the high-temperature dryout is slightly above 40 mm, which is consistent with the value calculated using the heat flux plate. The data from UT notches UT1-63 and UT1-75 would indicate that a bad signal was being received from the notch between them, causing one to indicate a high temperature, with an equivalent offset in the low direction on the other element.

The experimental operations performed during the second ACRR run are summarized in Table 8. At the conclusion of these

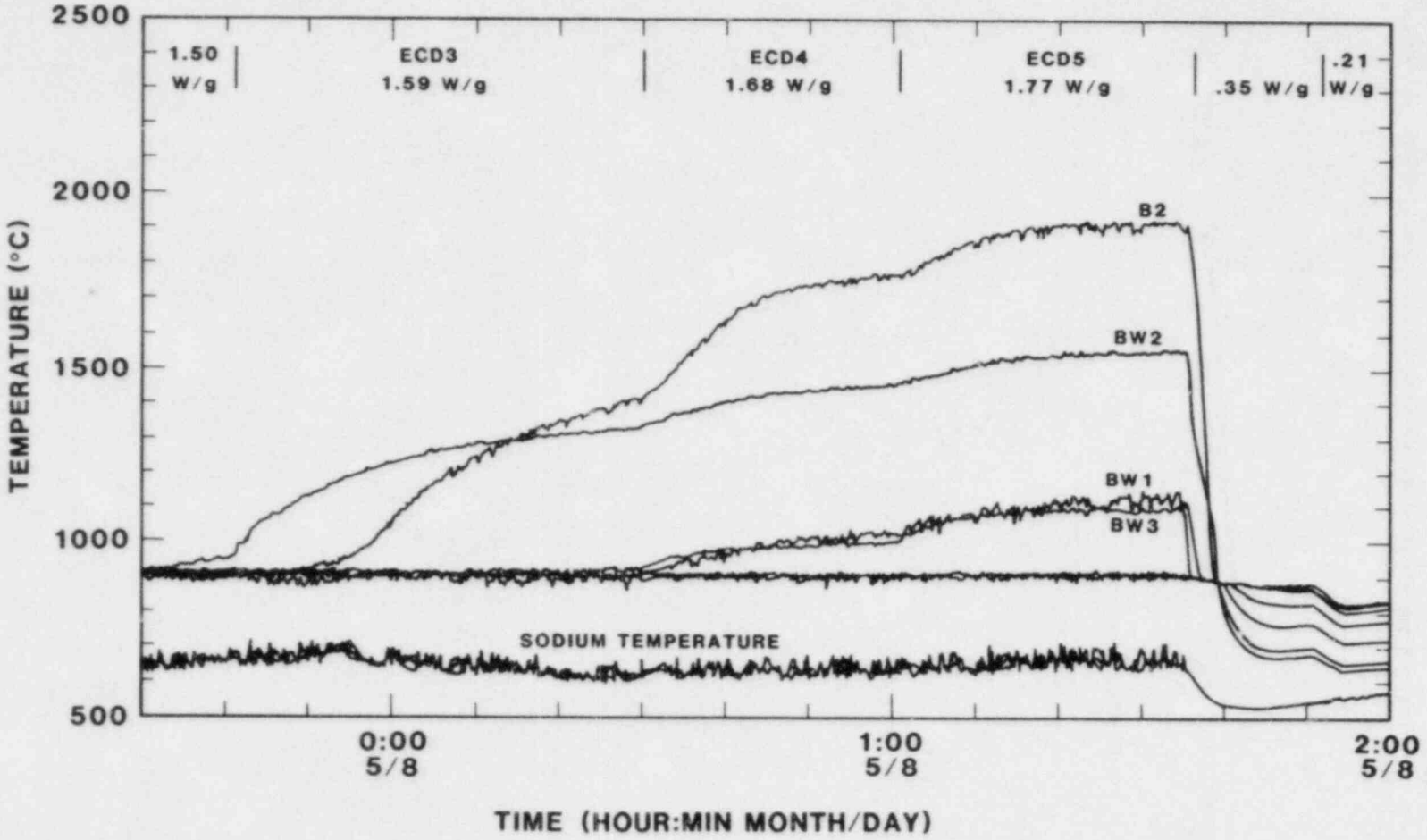

Figure 21. Postdryout in a Channeled Bed

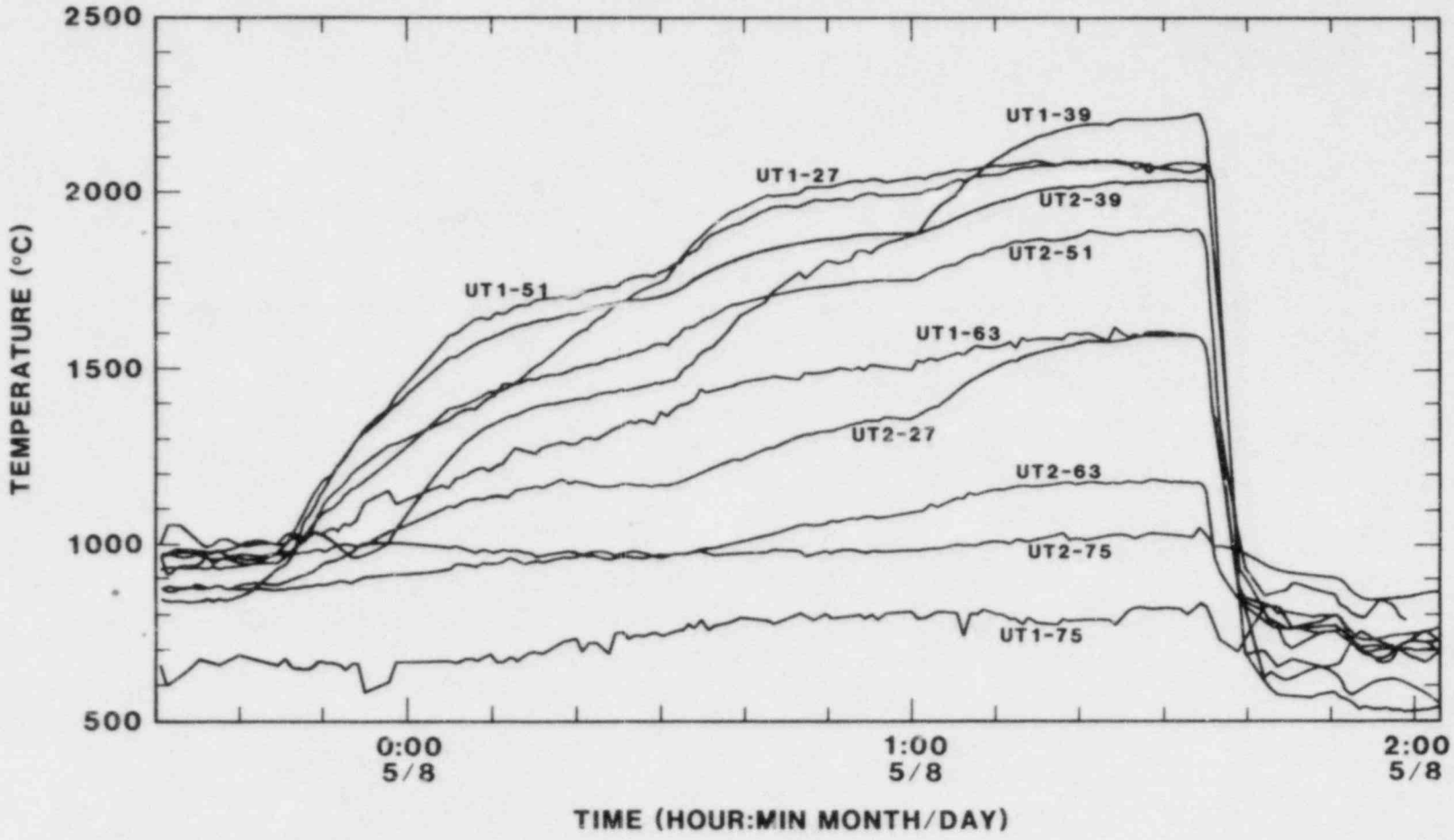

Figure 22. UT Data for ECD3, ECD4, ECD5

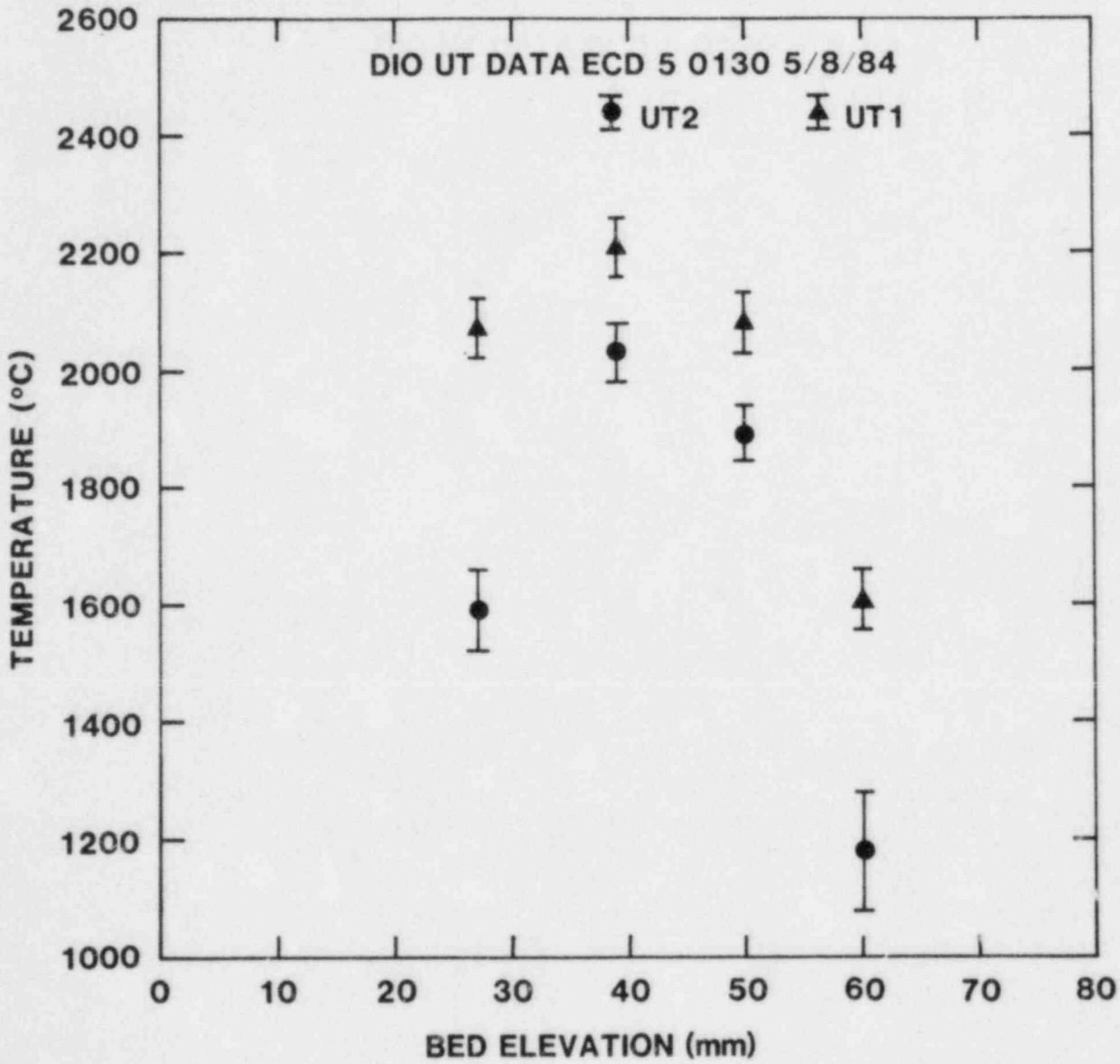

Figure 23. UT Data at the End of ECD5

Table 8

Additional Investigations (May 7 and 8)

Time	Event	Bed Power (W/g)	He Flow (g/s)	$Z_{a,c}$ (mm)	Sodium Temp (°C)	Max Bed Temp (°C)
1616	CR11	0.159	0		351	533
1618	PC4	0.531	0		351	
1819	CR12	0.248	0		354	821
1838	F1	0.425	0		356	902
1946	F2	0.372	0		363	874
2027	CR13	0.212	0		350	694
2044	F3	0.425	0		356	895
2118	PS1	01.77	0		415	1002
2127	F4	0.425	0		373	865
2212	F5	0.478	9.6		460	910
2340	ICD6	1.50	12.9		650	953
0030	ECD3	1.59	17.0	43	622	1418
0100	ECD4	1.68	17.6	42	630	1769
0134	ECD5	1.77	18.1	41	650	1909
0150	Q5	0.354	4.0		549	885
0209	CR14	0.319	4.7		594	853
0306	F6	0.425	5.3		569	921
0324	CR15	0.319	5.2		593	861
0411	CR16	0.159	0		352	588
0412	PC5	0.531	0		352	

F = Superheat flash

investigations, the bed appeared to have remained in a channeled configuration in spite of several attempts to reestablish a packed bed state. Since all planned objectives of the experiment had been achieved and it appeared that no additional useful data could be obtained, the experiment was concluded after more than 53 hr of nuclear operation and many additional hours of electrical heating and cooldown.

4. ANALYSIS REQUIREMENTS

The D10 experiment has provided much unique data in the field of debris coolability. The limited evaluations presented in this report provide some insight as to bed behavior with bottom cooling and at high temperatures; however, a more thorough understanding of heat transfer in the D10 bed will be gained only by additional, more complete analyses. The specific areas that would appear to be most valuable for continued analyses are identified and discussed in this section.

4.1 Bed Configuration

The configuration of the bed during the experiment, especially after the disruption event, is critical to more detailed analyses. It is important to establish the boundary conditions that are the basis for such analyses. The evaluation of the data so far would suggest that the disruption event increased the porosity only slightly. The x-ray of the bed taken after the experiment was completed indicates that the bed height varies rather uniformly from 164 to 170 mm, with an average height of 167 mm. This would indicate that the average porosity in the bed is about 0.40. However, the local porosity in the upper bed may be somewhat higher. A region in the bed extending from 20 to 60 mm, corresponding to the region of maximum temperatures, was evident in the x-ray with density variations that appeared slightly different from the remainder of the bed. Additional data on local porosity will be gained only by disassembly of the experiment, with detailed postirradiation examination (PIE). Since this information can be gained only at considerable expense, it will not be available for further analyses.

4.2 Data Interpretation with Respect to Current Models

Although current models are reasonably consistent with the data from D10 with the bed in a packed state, the data after the disruption event are not consistent with what would be predicted with a channeled model. Whether or not this is due to uncertainty in the bed configuration could be investigated parametrically with the models. There does, however, appear to be a fundamental discrepancy in the power calculated to be removed by channeling prior to dryout. It is apparent that the depth of channel penetration and the size and number of channels that are assumed in the model should be reevaluated in light of the D10 data.

4.3 Bed Cohesion

The "sticking factor," which appeared to suppress channeling until a substantial overpressure was built up in the bed, has a potentially large influence on the coolability of debris in accident scenarios. An increase in coolability by a factor of 2.5 was observed in D10. The cause of this cohesion should be

accomplished to determine the relevant mechanisms that influence the phenomenon. These mechanisms may include particle shape, bed porosity, subcooling, bed chemistry, and bed power. Time dependent aspects of these parameters should also be studied.

4.4 Dry Bed Thermal Conductivity

The conductivity of UO_2 debris with sodium vapor present is among the most significant data that will be obtained from the DlO experiment. Two-dimensional analysis conducted to date would indicate that the conductivity is significantly higher than models would predict. The mechanisms that might be responsible for the increase in conductivity are not clear at this time.

An important step in the continuation of this analysis is the ability to properly interpret the experimental data. This interpretation is dependent on the geometry of the dry zone, which affects heat transfer along the instrumentation. The determination of bed configuration will aid in this area. Furnace testing of instrumentation in environments that simulate the conditions that existed during the experiment may be helpful in assessing the data. Additional information may be gained by a study of the processes that might account for the observed increase in conductivity. These investigations should concentrate on those effects that might be related to the presence of sodium, since the models are consistent with the data for dry debris in argon, investigated in the SNL DC experiments (22). Based on a more detailed interpretation of the data, two- and three-dimensional thermal analyses should provide an important evaluation of the data in terms of mechanisms that could be responsible for enhanced conductivity. For example, radiation heat transfer should increase as the fourth power of temperature, conduction should be linear with temperature, and mass transport effects may be discernable.

5. SUMMARY AND CONCLUSIONS

The D10 experiment was the first fission-heated debris coolability experiment to study the effects of bottom cooling that might be provided by structural materials onto which the reactor debris might settle in an accident. In addition, it was successfully operated for more than 53 hr and achieved all experimental objectives, including operation at high temperatures in the debris, which approached the melting temperature of UO_2.

Downward cooling in a subcooled bed was investigated at power levels from 0.16 to 0.32 W/g with downward heat removal from 32% to 72% of the total bed power. Packed bed dryouts were achieved with a sodium subcooling of 500 K at powers ranging from 0.42 W/g to 0.58 W/g and downward cooling of 27% (120 kW/m^2) to 45% (260 kW/m^2). Channeling was induced after a disruption in the bed, which appeared to increase the bed porosity. Incipient channeled dryout power with a sodium subcooling of 370 K was 1.06 W/g and downward heat removal of 13% (140 kW/m^2). Extended dry zones were established at power levels of 1.6 W/g. The dry zone expanded more rapidly than models would have predicted; however, the dry zone conductivity appears to be higher than would be calculated with current models. Maximum bed temperatures of over 2500°C were achieved in a dry zone that was about 6 cm thick. This would indicate that UO_2 melting would have occurred at a power only slightly greater than 1.6 W/g.

A summary of the various experimental conditions is shown in Figure 24, with downward heat removal and temperature of the bottom of the bed as variables. Also plotted is the downward heat removal that would exist for steel plates 4 and 10 cm thick with a lower boundary temperature of 300°C. A wide range of downward cooling conditions was achieved during the experiment, ranging from 50 to 450 kW/m^2. Bed bottom temperatures as high as the sodium saturation temperature of 920°C were attained.

In the area of experimental capabilities, several noteworthy accomplishments were successfully attained after considerable effort in the preparation of the experiment. These included the successful development and operation of the Ta-10W high-temperature crucible, despite several temperature cycles through the recrystallization temperature; development of high-temperature thermocouples with 8 of 10 high-temperature thermocouples operating at the beginning of the experiment remaining operational, both UTs remaining operational, and both experiment radiological containment barriers remaining intact. Thus, in addition to the important data obtained for development of debris coolability models, it was demonstrated that experiments can be accomplished in which UO_2 is fission-heated to near UO_2 melt in the presence of sodium.

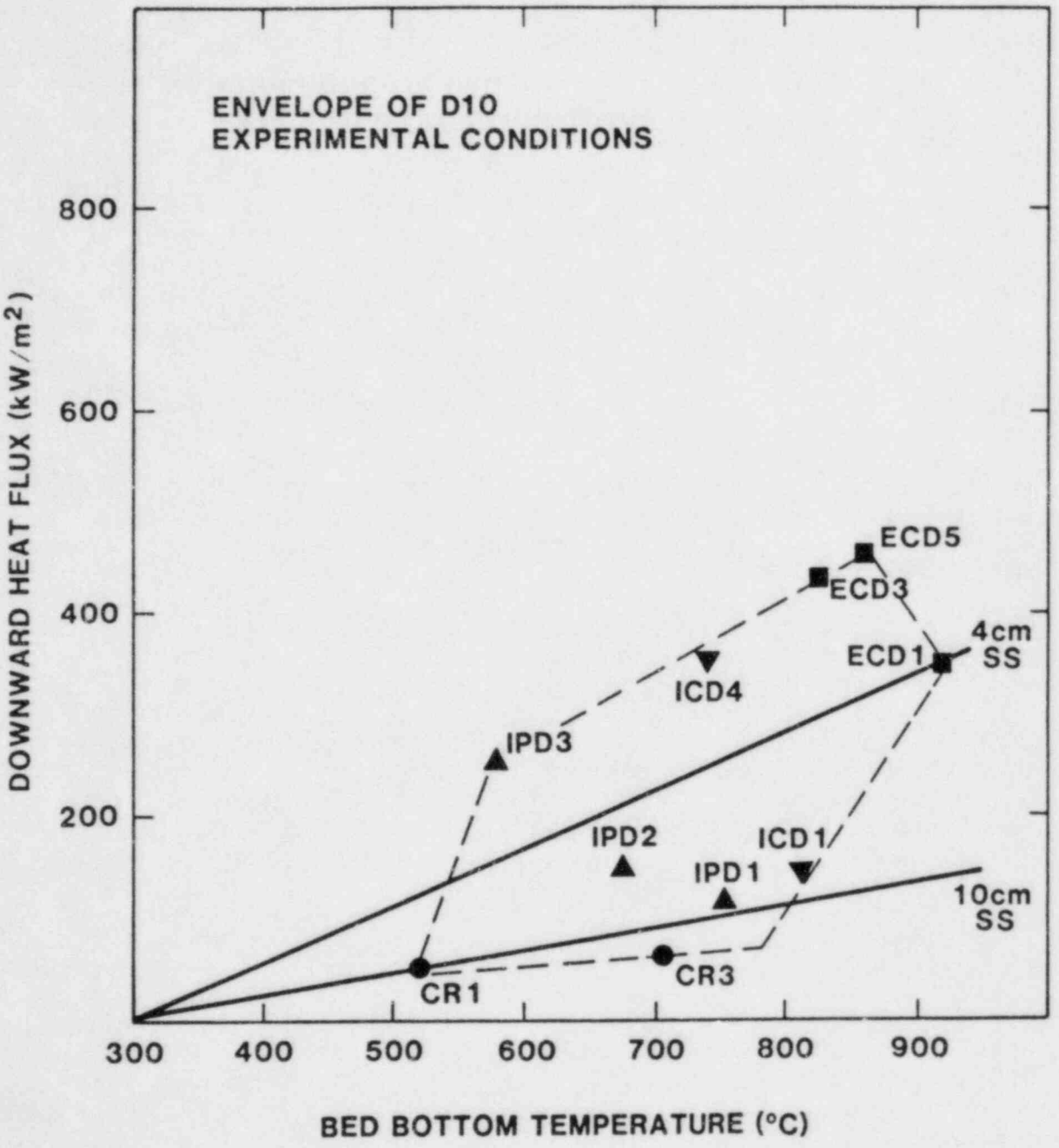

Figure 24. D10 Data Summary

6. REFERENCES

1. J. B. Rivard, Post-Accident Heat Removal: Debris Bed Experiments D-2 and D-3, NUREG/CR-0421, SAND78-1238, Sandia National Laboratories, Albuquerque, NM (1978).

2. E. Gronager, M. Schwarz, and R. J. Lipinski, PAHR Debris Bed Experiment D-4, NUREG/CR-1809, SAND80-2146, Sandia National Laboratories, Albuquerque, NM (1981).

3. G. W. Mitchell, R. J. Lipinski, and M. Schwarz, Heat Removal from a Stratified UO_2-Sodium Particle Bed, NUREG/CR-2412, SAND81-1622, Sandia National Laboratories, Albuquerque, NM (1982).

4. G. W. Mitchell, C. A. Ottinger, and R. J. Lipinski, The D7 Debris Bed Experiment, NUREG/CR-3198, SAND82-0062, Sandia National Laboratories, Albuquerque, NM (1983).

5. C. A. Ottinger, G. W. Mitchell, R. J. Lipinski, and J. E. Kelly, The D9 Experiment: Heat Removal from Stratified UO_2 Debris in Sodium, NUREG/CR-2951, SAND84-1838, Sandia National Laboratories, Albuquerque, NM (1984).

6. J. R. Koteras to G. W. Mitchell, "Evaluation of D10 Containment Vessels for Bottom Plate Operating Temperatures Between 700°C and 800°C", Sandia National Laboratories Internal Memorandum, December 7, 1983.

7. G. W. Fieg and H. Meister, "Thermal Analysis of D10 with the TAC-2D Code", Sandia National Laboratories Internal Memorandum, July 25, 1983.

8. "Program Plan for Selection of Refractory Materials for the D-10/D-13 Experiments," Internal Memorandum, Sandia National Laboratories, October 8, 1982.

9. Review Meeting, Joint Debris Coolability Program, Sandia National Laboratories, April 1983.

10. D. Clauss, Internal memorandum to G. Mitchell, "Structural Analysis of D10 Crucible," July 15, 1983.

11. Zircar Products Technical Data Bulletin No. ZPI 205, Aug 1, 1978.

12. J. B. Rivard et al, Feasibility of Bottom-Cooled Debris Experiments in the Annular Core Research Reactor, NUREG/CR-4254, SAND79-0876, Sandia National Laboratories, Albuquerque, NM (1980).

13. C. P. Cannon, "2200°C Thermocouples for Nuclear Reactor Fuel Centerline Temperature Measurements," in Temperature: Its Measurement and Control in Science and Industry, Volume 5, J. F. Schooley, ed, American Institute of Physics, New York, 1982.

14. C. P. Cannon, "Recent Advances in High Temperature Thermocouples," Proceedings of the Industrial Temperature Measurement Symposium, Knoxville, Tennessee; Sept 10-12, 1984.

15. M. E. Field, "Development of Ultrasonic Thermometry for Application in LMFBR Safety Research," Ultrasonic Symposium, Dallas, TX, November 13-16, 1984.

16. C. J. Greenholt and R. A. Sallach, memo to J. E. Gronager, "Water Adsorption by the Urania Bed in the D-Series Crucible ACRR Program," February 1, 1983.

17. T. R. Schmidt, memo to G. W. Mitchell, "Power Distribution in the D-10 Debris Bed Experiment," July 11, 1984.

18. K. Mehr, private communication.

19. L. Barleon, K. Thomauske, and H. Werle, Nucl Tech, 65, 67-86, (1984).

20. R. J. Lipinski, Nucl Tech, 65, 53-66, (1984).

21. H. Nakamura, "Analysis of Temperatures in D10 Dryout Zones due to Instrumentation," Sandia National Laboratories Internal Memorandum, October 20, 1983.

22. J. T. Hitchcock and J. E. Kelly, The DC1 and DC2 Debris Coolability Experiments, NUREG/CR-4060, SAND84-1367, Sandia National Laboratories, Albuquerque, New Mexico (to be published).

APPENDIX A

Experiment Design Drawings

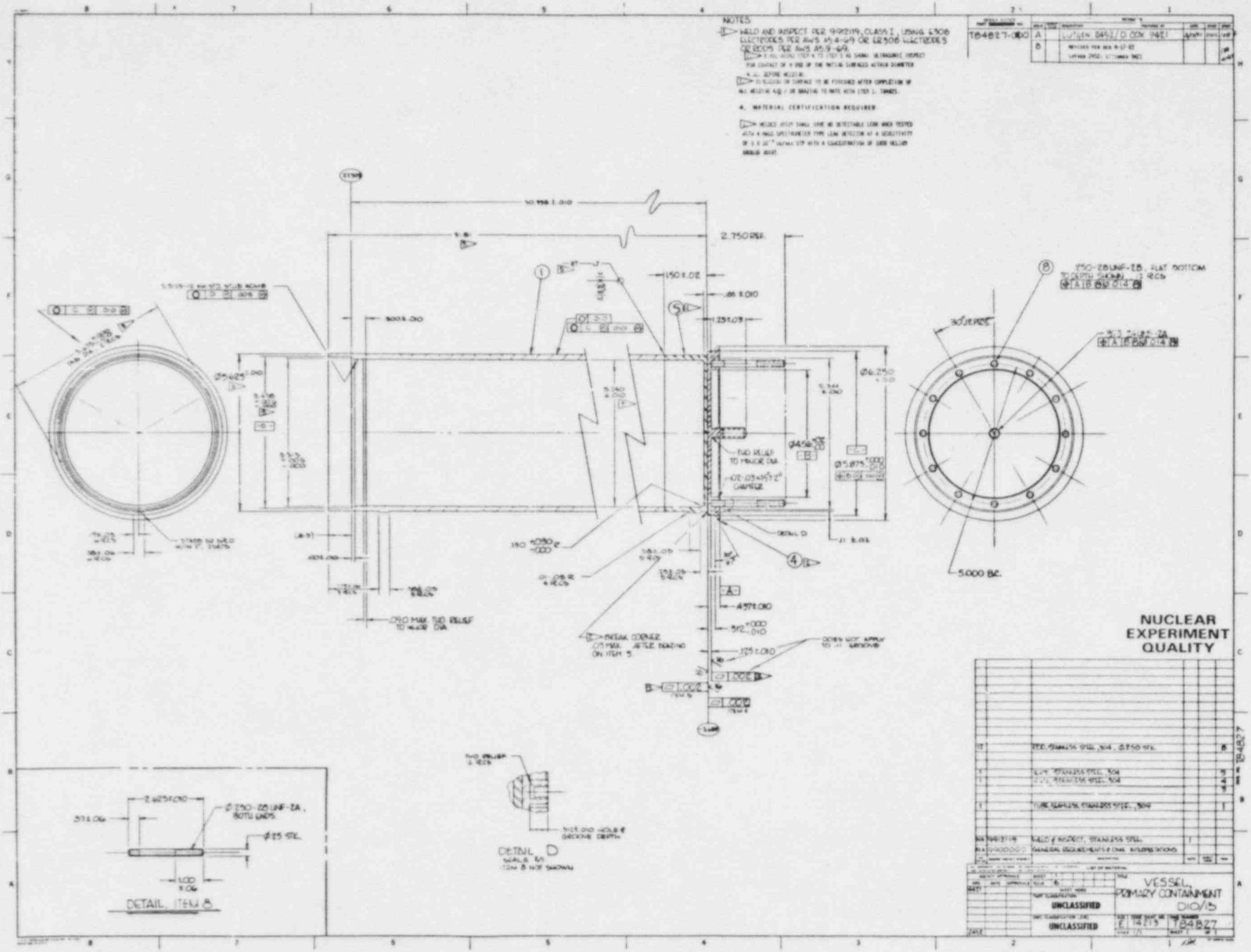
NOTES
NUCLEAR EXPERIMENT QUALITY
DETAIL ITEM 8
DETAIL D
VESSEL, PRIMARY CONTAINMENT
UNCLASSIFIED
UNCLASSIFIED
184827

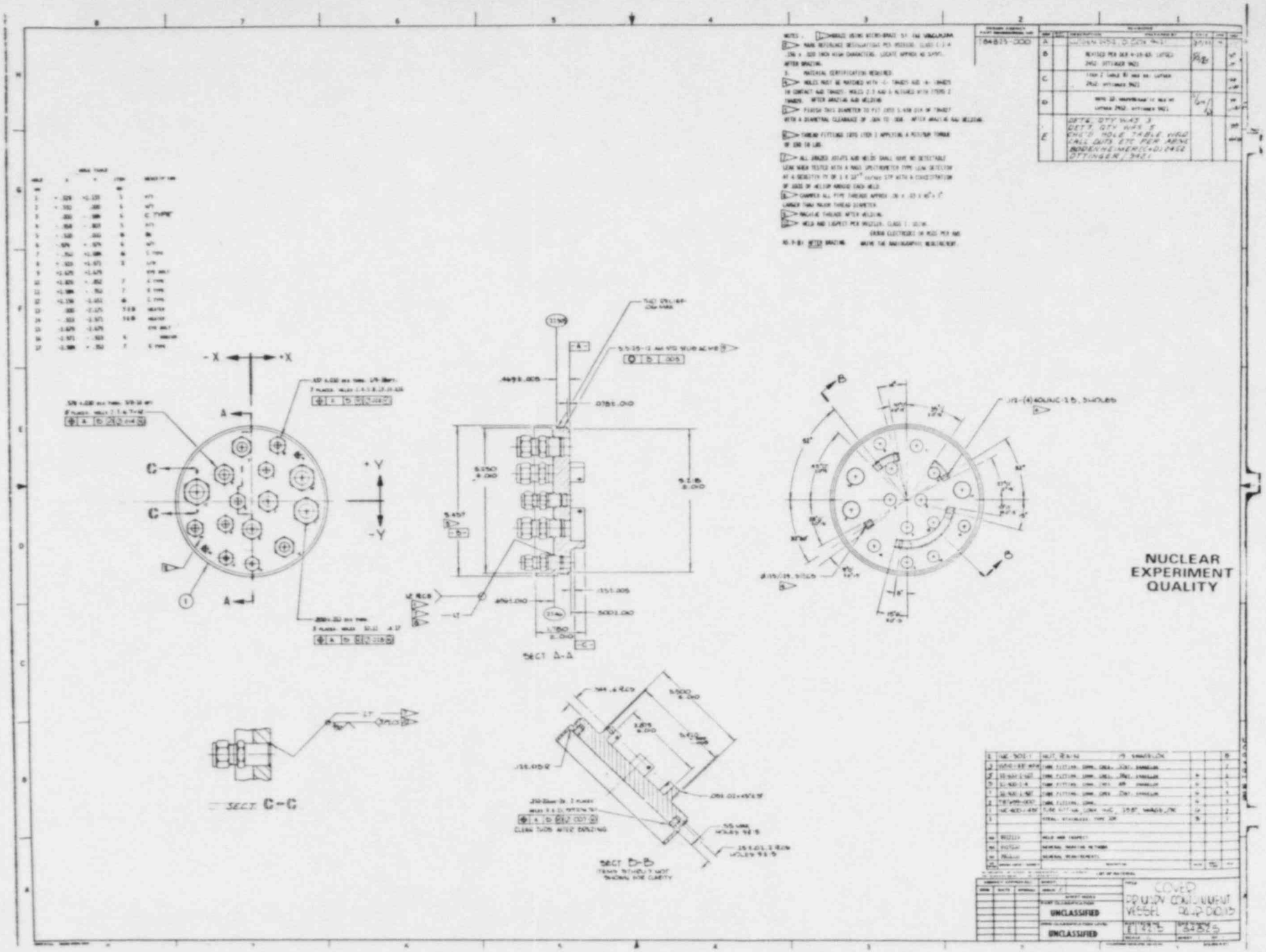
NUCLEAR
EXPERIMENT
QUALITY
SECT A-A
SECT B-B
SECT C-C
UNCLASSIFIED
UNCLASSIFIED

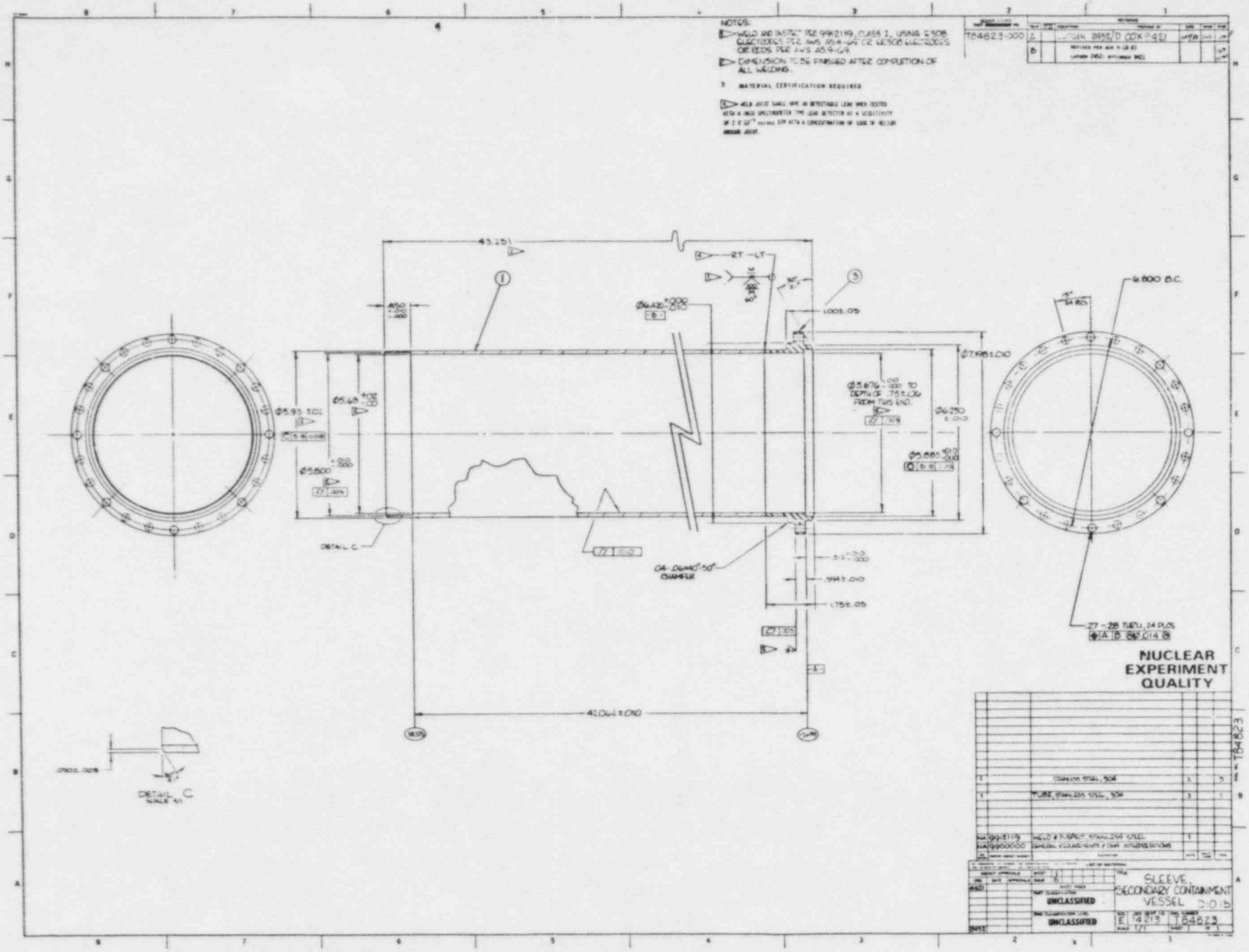
NOTES:
1. WELD AND INSPECT PER 99K2119, CLASS I, USING E308 ELECTRODES PER AWS A5.4-69 OR E308 ELECTRODES OR RODS PER AWS A5.9-69.
2. DIMENSION TO BE FINISHED AFTER COMPLETION OF ALL WELDING.
3. MATERIAL CERTIFICATION REQUIRED
4. WELD JOINT SHALL NOT BE DETECTABLE LEAK WHEN TESTED WITH A MASS SPECTROMETER TYPE LEAK DETECTOR AT A SENSITIVITY OF 2 X 10⁻⁶ STD. CC/SEC. HE WITH A CONCENTRATION OF 1000 PPM HELIUM MINIMUM.
T84823-300
43.251
RT - LT
Ø6.420 +.000 -.010
1.003±.015
Ø7.998±.010
Ø5.676 +.000 -.000 TO DEPTH OF .75±.06 FROM THIS END.
Ø6.250 ±.010
Ø5.885 +.010 -.000
Ø5.93 ±.01
Ø5.60 +.02 -.00
Ø5.800 +.000 -.010
DETAIL C
.04 - .060" x 30° CHAMFER
.511 +.010 -.000
.994±.010
.756±.05
42.064±.010
6.800 B.C.
.5" 14 RDS
27 - 28 TUBES, 24 PLUS
⌖ A B Ø.010 B
DETAIL C
SCALE 4/1
NUCLEAR EXPERIMENT QUALITY
T84823
SLEEVE, SECONDARY CONTAINMENT VESSEL D.O.E.
UNCLASSIFIED
UNCLASSIFIED
E 4219
T84823

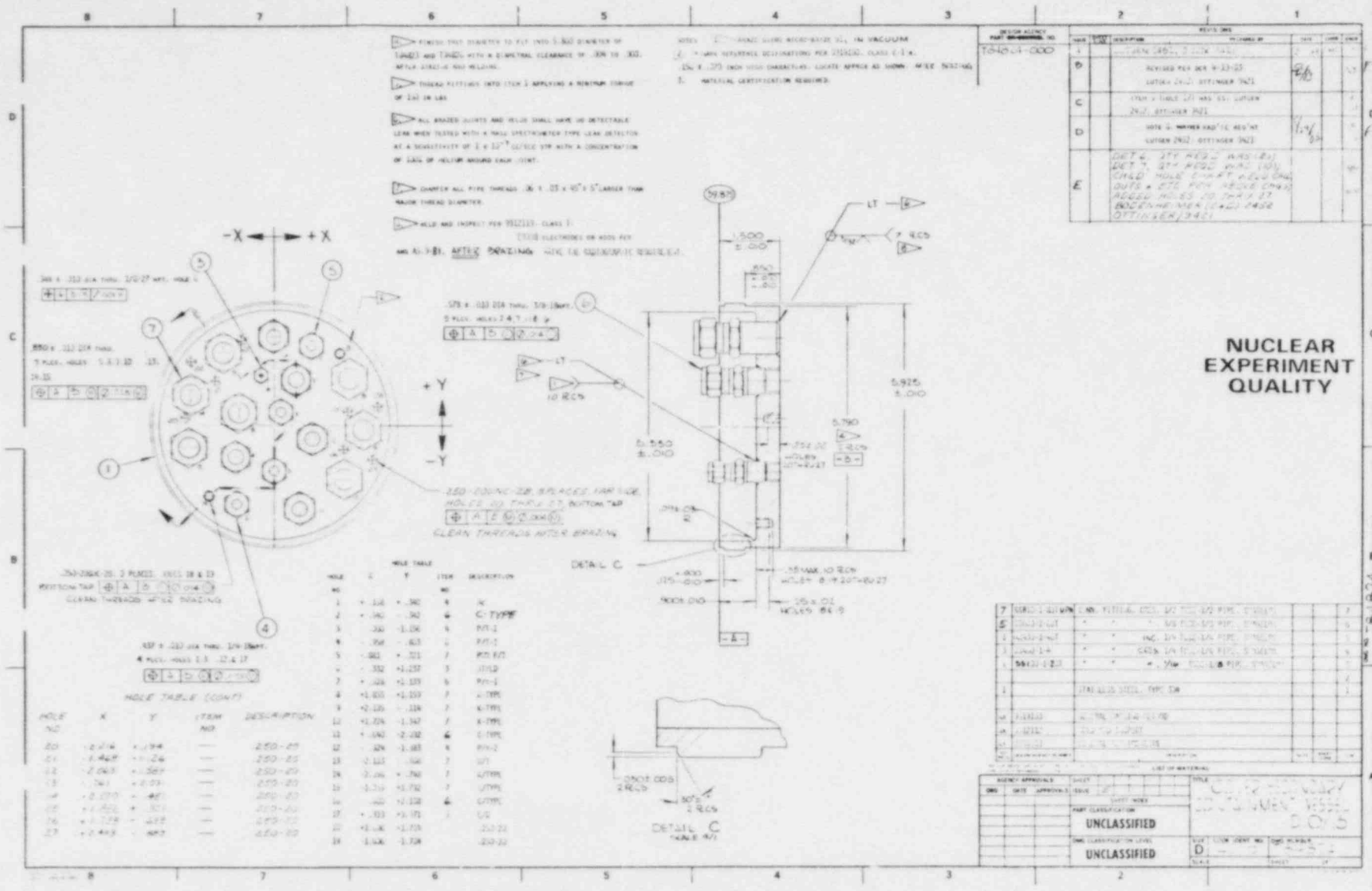
NUCLEAR
EXPERIMENT
QUALITY
UNCLASSIFIED
UNCLASSIFIED
DETAIL C
SCALE 4/1
HOLE TABLE
HOLE TABLE (CONT)

APPENDIX B

Bed Power Distribution

Height (cm)								
15.2	1.06×10^{-5}	1.05×10^{-5}	1.05×10^{-5}	1.06×10^{-5}	1.08×10^{-5}	1.09×10^{-5}	1.09×10^{-5}	1.12×10^{-5}
13.6	9.49×10^{-6}	9.51×10^{-6}	9.55×10^{-6}	9.66×10^{-6}	9.77×10^{-6}	9.95×10^{-6}	1.02×10^{-5}	1.07×10^{-5}
12.0	9.58×10^{-6}	9.60×10^{-6}	9.66×10^{-6}	9.75×10^{-6}	9.90×10^{-6}	1.10×10^{-5}	1.04×10^{-5}	1.09×10^{-5}
10.4	9.66×10^{-6}	9.70×10^{-6}	9.75×10^{-6}	9.85×10^{-6}	1.00×10^{-5}	1.02×10^{-5}	1.05×10^{-5}	1.10×10^{-5}
8.8	9.75×10^{-6}	9.80×10^{-6}	9.85×10^{-6}	9.95×10^{-6}	1.00×10^{-5}	1.02×10^{-5}	1.05×10^{-5}	1.10×10^{-5}
7.2	9.73×10^{-6}	9.75×10^{-6}	9.83×10^{-6}	9.93×10^{-6}	1.00×10^{-5}	1.00×10^{-5}	1.05×10^{-5}	1.10×10^{-5}
5.6	9.64×10^{-6}	9.63×10^{-6}	9.74×10^{-6}	9.85×10^{-6}	9.96×10^{-6}	1.00×10^{-5}	1.04×10^{-5}	1.09×10^{-5}
4.0	9.49×10^{-6}	9.53×10^{-6}	9.56×10^{-6}	9.68×10^{-6}	9.84×10^{-6}	1.00×10^{-5}	1.03×10^{-5}	1.07×10^{-5}
2.4	9.18×10^{-6}	9.21×10^{-6}	9.27×10^{-6}	9.37×10^{-6}	9.53×10^{-6}	9.77×10^{-6}	1.00×10^{-5}	1.05×10^{-5}
0.8	8.8×10^{-6}	8.89×10^{-6}	8.92×10^{-6}	9.31×10^{-6}	9.14×10^{-6}	9.36×10^{-6}	9.67×10^{-6}	1.01×10^{-5}

59,60

Figure B-1. D10 Bed Power Distribution

APPENDIX C

Experimental Procedures

D10 EXPERIMENTAL PROCEDURES

Startup

1. Electrically heat the sodium to 350°C. Do not exceed 35 V electrical power until sodium is at 120°C at S5.

2. Nuclear heating of the debris bed following melting of the sodium at a power of about 0.2 W/g (90 kW ACRR power).

Control Run

3. Initiate upward (nitrogen) cooling sufficient to maintain a sodium temperature of 350°C for a control run. No helium mass flow (minimum bottom cooling) would be used although there would be a finite downward heat flux. ACRR power should be adjusted to achieve a maximum bed temperature of about 600°C. This power level is henceforward referred to as control run power.

   Analyst - Determine bed conductivity vs elevation.

Power Calibration

4. A power calibration run to establish the ratio of bed power to ACRR power, which is continuously recorded, would be accomplished by rapidly increasing power to 300 kW (600 kW scale), maintaining 300 kW for a period of about 2 min, and then reducing it back to the control run power.

   Analyst - Determine coupling factor.

Wetting of UO_2

5. Wetting of the UO_2 by the sodium is desirable to release trapped gas and ensure a stable thermal response of the bed throughout the experiment. Wetting occurs more readily at high temperatures. Therefore, to achieve wetting, increase sodium temperature to 600°C using both electrical and nuclear heating. Adjust power to ensure that maximum bed temperatures are less than 800°C. Helium cooling flow would be as low as possible but sufficient to maintain containment temperatures below 700°C. Hold maximum temperatures for 1 hr. This procedure also serves as a 600°C control run.

   Analyst - Determine bed conductivity vs elevation, compare conductivity from step 3. Determine downward heat flux at zero and minimum controllable (approximately 10 lb/hr) flow as a function of fin and containment temperatures.

Conduction/Single-Phase Convection

6. In order to establish various subcooled temperature profiles in the bed at different amounts of downward heat removal, increase downward cooling to 30, 60, and 120 lb/hr constant bed power and a sodium temperature of 600°C.

   Analyst - Determine helium cooling capability as a function containment temperatures.

7. At a sodium temperature of 600°C and at 120 lb/hr helium flow, increase bed power until maximum temperatures are near 800°C.

   Analyst - Helium cooling vs containment temperature.

8. Reduce bed power to the control run power (90 kW). Reduce sodium temperature to 350°C, maintaining 120 lb/hr helium flow.

9. Decrease downward cooling to 60, 30, and minimum achievable, at constant bed power, and at a sodium temperature of 350°C. (Second 350°C control run.)

   Analyst - Determine bed conductivity vs elevation. Compare with previous data, provide to experimenter.

10. Conduct second power calibration at 350°C (90 to 300 kW).

    Analyst - Determine coupling factor.

11. Increase power in two steps at minimum downward cooling to establish stable temperature profiles with maximum temperatures between 750° and 800°C.

Two-Phase Heat Removal/Packed Bed Incipient Dryout

12. In order to study heat transfer by boiling, establish the allowable downward heat flow as dictated by temperature limits and increase power until boiling is observed (about 850°C). Increase power in two steps to establish thicker stable regions.

    Analyst - Determine desired power steps.

13. Continue to increase power until dryout is observed and until dryout extends to the walls of the crucible. To maintain crucible and instrumentation temperatures well within their capabilities, limit crucible wall temperature to about 1000°C and the maximum bed temperature to about 1800°C. If channeling is observed before reaching a packed bed dryout temperature of 1800°C, reduce power to reestablish a packed bed dryout and continue to step 14.

Analyst - Using this data and that from steps 16, 19, and 22, determine the conductivity of the dry zone vs temperature, and estimate the power required to achieve bed temperatures of 2600°C for both packed and channeled conditions.

14. Increase downward cooling to quench dryout and reduce the size of the boiling region.

15. Repeat steps 13 and 14 at 30, 60, and 120 lb/hr helium cooling until the maximum available downward cooling is achieved.

Channeling Penetration and Channeled Dryout Investigations

16. If channeling has not already occurred at a sodium temperature of 350°C, establish the lowest allowable downward heat removal as dictated by containment temperatures and increase power to establish a small dry zone. Increase power rapidly to 1.5 times the dryout power. Maintain and observe for channel penetration. Limit bed and crucible wall temperatures to 1800° and 1000°C. If not observed, return to a small dry zone and repeat at 2.0 times dryout power. Continue increasing power steps until channel penetration is observed; then adjust power downward to reestablish packed bed dryout so as to accurately determine power required for channel penetration.

NOTE:
If the dryout is quenched by channel penetration, increase power rapidly but in small steps, limiting maximum power to 2.0 W/g. Maintain at maximum power for 10 min if dryout is not observed, then reduce power to maintain but reduce the extent of the boiling region.

17. Repeat Step 16 at 120 lb/hr helium flow.

18. Reduce downward cooling to the minimum achievable. Reduce power to limit the extent of the boiling/dry region. Reduce cooling or increase electrical heater power to increase sodium temperature to 600°C.

Subcooling Effects on Packed Bed Dryout

19. At a sodium temperature of 600°C, increase bed power at the allowable bottom cooling until dryout is observed and extends to the crucible walls. Limit wall and bed temperature to 1000° and 1800°C. If channel penetration occurs, power to reestablish packed bed dryout and continue to step 20.

20. Increase downward cooling to quench dryout and reduce the size of the boiling region.

21. Repeat steps 19 and 20 at 30, 60, and 120 lb/hr helium flow rate.

Subcooling Effects on Channeling

22. If channeling has not already occurred at a sodium temperature of 600°C, establish the lowest allowable downward heat removal and increase power to establish a small dry zone. Increase power rapidly to 1.5 times the dryout power. Limit crucible and bed temperatures to 1000° and 1800°C. If channeling is not observed, return to a small dryout and increase power to 2 times the dryout power. Continue increasing power until channeling is observed, then adjust power downward to reestablish packed dryout so as to accurately determine channel penetration criteria.

NOTE:
If the dryout is quenched by channel penetration, increase power rapidly but in small steps, limiting maximum power to 2.0 W/g. Maintain at maximum power for 10 min if dryout is not observed, then reduce power to reduce the extent of the boiling region.

23. Repeat step 22 at maximum downward cooling.

24. Reduce downward cooling to the minimum achievable. Reduce to limit the extent of the boiling/dry zone. Increase nitrogen cooling to cool sodium to 350°C.

Extended Dryout

25. Reduce sodium temperature to 350°C. Maintain boiling at lowest downward cooling. Increase power to establish small dry zone. Increase power rapidly to a power to establish a thick dry zone in a single step. Limit crucible and containment temperature to maximum allowable. Adjust power to achieve maximum bed temperature (~2600°C). Hold maximum temperature for 2 hr.

Analyst - Determine power required to reach 2600°C.

26. Increase sodium temperature to 600°C. Maintain dry zone maximum temperature at 2600°C. Hold for 2 hr.

27. Increase downward cooling by about 50%. Increase power to maintain a maximum dry zone temperature of 2600°C.

28. Reduce power in three or four steps until dryout is quenched.

29. Increase power in three or four steps to reestablish a 2600°C dry zone at minimum downward cooling.

Control Run

30. Cool sodium to 350°C. Establish a nonboiling control run.

31. Conduct third power calibration at 350°C.

D10 RERUN PROCEDURES

1. Electrical heating

2. 350°C sodium, 90-kW control run

3. Power calibration 90-300-180 kW

4. Increase power in 30-kW steps. If dryout occurs at less than 300 kW, proceed to step 15.

5. Reduce power to 150 kW and subcool sodium 30 degrees.

6. Increase power in 30-kW steps. If dryout occurs at less than 300 kW, proceed to step 13.

7. Reduce power to 120 kW and subcool sodium 100 degrees.

8. Increase power in 30-kW steps. If dryout occurs at less than 300 kW, proceed to step 13.

9. Reduce power to 120 kW and subcool sodium 100 degrees.

10. Increase power to 1.0 MW, limit crucible wall temperatures to 1200°C.

11. Reduce power to 210 kW to reestablish a boiling state.

12. Increase power in 30-kW steps. If dryout occurs at less than 300 kW, proceed to step 15. If not, return to 90-kW control run.

    Note: The following procedures assume that the bed remains in a packed state. If channeling occurs, return to step 5 to reestablish a packed state and then resume the experiment.

13. Increase power in two 30-kW steps to establish stable dry zones. Limit crucible wall temperatures to 1200°C.

14. Quench dry zone by returning to incipient boiling power.

15. Increase sodium temperature to 600°C.

16. Increase power in 30-kW steps to find packed bed incipient dryout for 600°C sodium.

17. Increase power in two 30-kW steps above incipient dryout to establish stable dry zones. Limit wall to 1200°C.

18. Quench dry zone by decreasing power to between boiling and dryout power. Increase helium flow to 100 lb/hr.

19. Increase power in 30-kW steps to find incipient dryout. Increase power in two 30-kW steps above dryout. Limit wall temperatures to 1200°C.

20. Quench dryout by decreasing power to between boiling and dryout power. Increase nitrogen flow to cool sodium to 350°C.

21. Increase power to 30-kW steps to find incipient dryout. Increase power in two 30-kW steps above dryout. Limit wall temperatures to 1200°C.

22. Reduce power to 120 kW. When a stable subcooled state has been reached, increase power to 1 MW. Limit crucible wall temperatures to 1200°C.

23. Reduce power to 180 kW. Increase sodium temperature to 600°C.

24. Reduce power to 120 kW. When a stable subcooled state has been reached, increase power to 1 MW. Limit crucible wall temperatures to 1200°C.

25. Establish 90-kW control run.

DISTRIBUTION:

Division of Technical Information and Document Control
NRC Distribution Contractor
U.S. Nuclear Regulatory Commission
15700 Crabbs Branch Way
Rockville, MD 20850
(250 copies for R7)

Division of Reactor Safety Research (8)
Office of Nuclear Regulatory Research
U.S. Nuclear Regulatory Commission
Washington, DC 20555
Attn: C. N. Kelber
M. Silberberg
R. W. Wright (5)
G. Marino

Joint Research Center (10)
Ispra Establishment
21020 Ispra (Varese)
Italy
Attn: R. Klersy
H. Holtbecker
D. Schwalm
K. Mehr
P. Fasoli-Stella
O. Simoni (5)
P. Schiller

Power Reactor & Nuclear Fuel (6)
Development Corporation (PNC)
Fast Breeder Reactor Development Project (FBR)
9-13, 1-Chome, Akasaka
Minato-Ku, Tokyo
Japan
Attn: Mochizuki
A. Watanabe (2)
H. Nakamura
M. Saito
K. Takahashi

Monsieur A. Schmitt
IPSN/DSN
CEN Fontenay-aux-Roses
B. P. 6
92260 Fontenay-aux-Roses
France

DISTRIBUTION (Continued)

Safety Studies Laboratory/DSN (5)
Commissariat a L'Energie Atomique
Centre d'Etudes Nucleaires de Cadarache
B. P. 1, 13115 Saint-Paul-lez-Durance
Bouches-du-Rhone
France
Attn: M. Schwarz
M. Bailly
M. Meyer Heine
M. Penet
G. Kayser
C. LeRigoleur

Centre d'Etudes Nucleaires de Grenoble (2)
B. P. 85-Centre de Tri
38401 Grenoble Cedex
Franch
Attn: M. Costa/STT
D. Rousseau/Pi-SEDTI

UKAEA (4)
Safety and Reliability Directorate
Wigshaw Lane
Culcheth
Warrington, WA3 4NE
England
Attn: M. Hayns
R. S. Peckover
B. D. Turland
K. A. Moore

Atomic Energy Establishment (5)
Winfrith, Dorchester
Dorset
United Kingdom
Attn: R. V. Macbeth
R. Potter
G. L. Shires
G. F. Stevens
R. Trenberth

Culham Laboratory (1)
Culham
Abingdon
Oxfordshire OX14 3DB
England
Attn: F. Briscoe

DISTRIBUTION (Continued)

Kernforschungszentrum Karlsruhe (8)
D-75 Karlsruhe
Postfach 3640
West Germany
Attn: G. Heusener (PSB)
P. Hoffmann (PSB)
H. Werle (INR)
L. Barleon (IRB)
G. Hoffman (IRM)
K. Thomauske (IRB)
U. Muller (IRM)
G. Fieg (INR)

University of California (4)
Energy and Kinetics Department
Rm. 5405 Bolter Hall
Los Angeles, CA 90024
Attn: I. Catton (2)
V. K. Dhir (2)

Argonne National Laboratory (5)
Reactor Analysis and Safety Division
9700 South Cass Avenue
Argonne, IL 60439
Attn: L. Baker, Jr.
J. C. Cassulo
J. D. Gabor
R. D. Pedersen
E. S. Sowa

Westinghouse Electric Corp. (1)
Power Systems
P.O. Box 355
Pittsburgh, PA 15230
Attn: L. Hochreiter

Westinghouse Research and Development Center (1)
Pittsburgh, PA 15235
Attn: A. Pieczynski

Westinghouse Hanford Co. (2)
337 Bldg., 300 Area
P.O. Box 1970
Richland, WA 99352
Attn: G. R. Armstrong
C. P. Cannon

Nuclear Safety Analysis Center (2)
3412 Hillview Avenue
P.O. Box 10412
Palo Alto, CA 94303
Attn: D. Squarer
G. Thomas

DISTRIBUTION (Continued)

Fauske and Associates (2)
631 Executive Dr.
Willowbrook, IL 60521
Attn: M. Epstein
R. Henry

Brookhaven National Laboratory (2)
Fast Reactor Safety
Upton, Long Island, NY 11973
Attn: J. W. Yang
T. Ginsberg

Los Alamos National Laboratory
Q7, Slot K556
Los Alamos, NM 87545
Attn: Javiei Escamilla

NUS Corporation
Consulting division
4 Research Place
Rockville, MD 20850
Attn: Juan M. Nieto

EG&G, Idaho (5)
P.O. Box 1625
Idaho Falls, ID 83415
Attn: C. Allison
T. M. Howe
T. S. Hsieh
R. J. Lloyd
R. W. Miller
B. J. Buescher

Mass. Inst. of Tech. (2)
Mech. Eng. Dept.
Cambridge, MA 02139
Attn: P. Griffith
M. Kazimi

University of New Mexico
Nuclear Engineering Department
Albuquerque, NM 87131
Attn: M. El-Genk

University of Wisconsin (2)
Department of Nuclear Engineering
Madison, WI 53706
Attn: M. Corradini
S. Abdel-Khalik

DISTRIBUTION (Continued)

Purdue University
Department of Nuclear Engineering
West Lafayette, IN 47907
Attn: T. Theofanous

Sandia National Laboratories:

1523 R. C. Reuter
1846 R. K. Quinn
3141 C. M. Ostrander (5)
3151 W. L. Garner
6400 A. W. Snyder
6410 J. W. Hickman
6420 J. V. Walker (5)
6421 T. R. Schmidt (5)
6421 K. R. Boldt
6421 D. N. Cox
6421 R. D. Gomez
6421 H. Meister (3)
6421 G. W. Mitchell (5)
6421 C. A. Ottinger (3)
6422 D. A. Powers
6423 P. S. Pickard
6423 A. Furutani
6425 W. J. Camp
6425 J. E. Kelly
6425 A. W. Reed
6427 M. Berman
6427 J. T. Hitchcock
6430 N. Ortiz
6440 D. A. Dahlgren
6450 J. A. Reuscher
6451 T. F. Luera
6452 M. F. Aker
6454 G. L. Cano
8024 M. A. Pound

NRC FORM 335 (2.84) NRCM 1102, 3201, 3202

U.S. NUCLEAR REGULATORY COMMISSION

BIBLIOGRAPHIC DATA SHEET

SEE INSTRUCTIONS ON THE REVERSE

1. REPORT NUMBER (Assigned by TIDC add Vol. No., if any)

NUREG/CR-4055
SAND84-1144

2. TITLE AND SUBTITLE

The D10 Experiment: Coolability of UO_2 Debris in Sodium with Downward Heat Removal

3. LEAVE BLANK

4. DATE REPORT COMPLETED

MONTH	YEAR
November	1984

5. AUTHOR(S)

G. W. Mitchell
C. A. Ottinger

6. DATE REPORT ISSUED

MONTH	YEAR
December	1984

7. PERFORMING ORGANIZATION NAME AND MAILING ADDRESS (Include Zip Code)

Degraded Core Coolability
Studies Division 6421
Sandia National Laboratories
Albuquerque, New Mexico 87185

8. PROJECT/TASK/WORK UNIT NUMBER

9. FIN OR GRANT NUMBER

A-1181

10. SPONSORING ORGANIZATION NAME AND MAILING ADDRESS (Include Zip Code)

Nuclear Regulatory Research
U.S. Nuclear Regulatory Commission
Washington, DC 20555

11a. TYPE OF REPORT

Technical

b. PERIOD COVERED (Inclusive dates)

January 1981-May 1984

12. SUPPLEMENTARY NOTES

13. ABSTRACT (200 words or less)

The LMFBR Debris Coolability Program at Sandia National Laboratories investigates the coolability of particle beds which may form following a severe accident involving core disassembly in a nuclear reactor. The D series experiments utilize fission heating of fully enriched UO_2 particles submerged in sodium to realistically simulate decay heating. The D10 experiment is the first in the series to study the effects of bottom cooling of the debris which could be provided in an actual accident condition by structural materials onto which the debris might settle. Additionally, the D10 experiment was designed to achieve maximum temperatures in the debris approaching the melting point of UO_2. The experiment was successfully operated for over 50 hours and investigated downward heat removal in a packed bed at specific powers of 0.16 to 0.58 W/g. Dryout in the debris was achieved at powers from 0.42 to 0.58 W/g. Channels were induced in the bed and channeled bed dryout was achieved at powers of 1.06 to 1.77 W/g. Maximum temperatures in excess of 2500°C were attained.

14. DOCUMENT ANALYSIS - a. KEYWORDS/DESCRIPTORS

b. IDENTIFIERS/OPEN-ENDED TERMS

15. AVAILABILITY STATEMENT

Unlimited

16. SECURITY CLASSIFICATION

(This page)

U

(This report)

U

17. NUMBER OF PAGES

72

18. PRICE